Bestimmung der Analysierstärke des A4-Compton-Rückstreupolarimeters

–

Determination of the analyzing power of the A4 Compton Backscattering Polarimeter

Jürgen Diefenbach

1. Juli 2010

MAMI – The Mainz Microtron Facility

Parity Violation in Elastic Electron Scattering

Compton Polarimetry

Experimental Realization

Data Analysis

Summary and Outlook

MAMI – The Mainz Microtron Facility

MAMI – beam parameters

- continuos (polarized) electron beam (coincidence experiments!)
- beam energy: 180...1508 (1558) MeV
- beam current up to 100 μA (polarized)
- “parity beam” at 315, 420, 510, 570, 855, 1500 MeV

MAMI – principle of operation

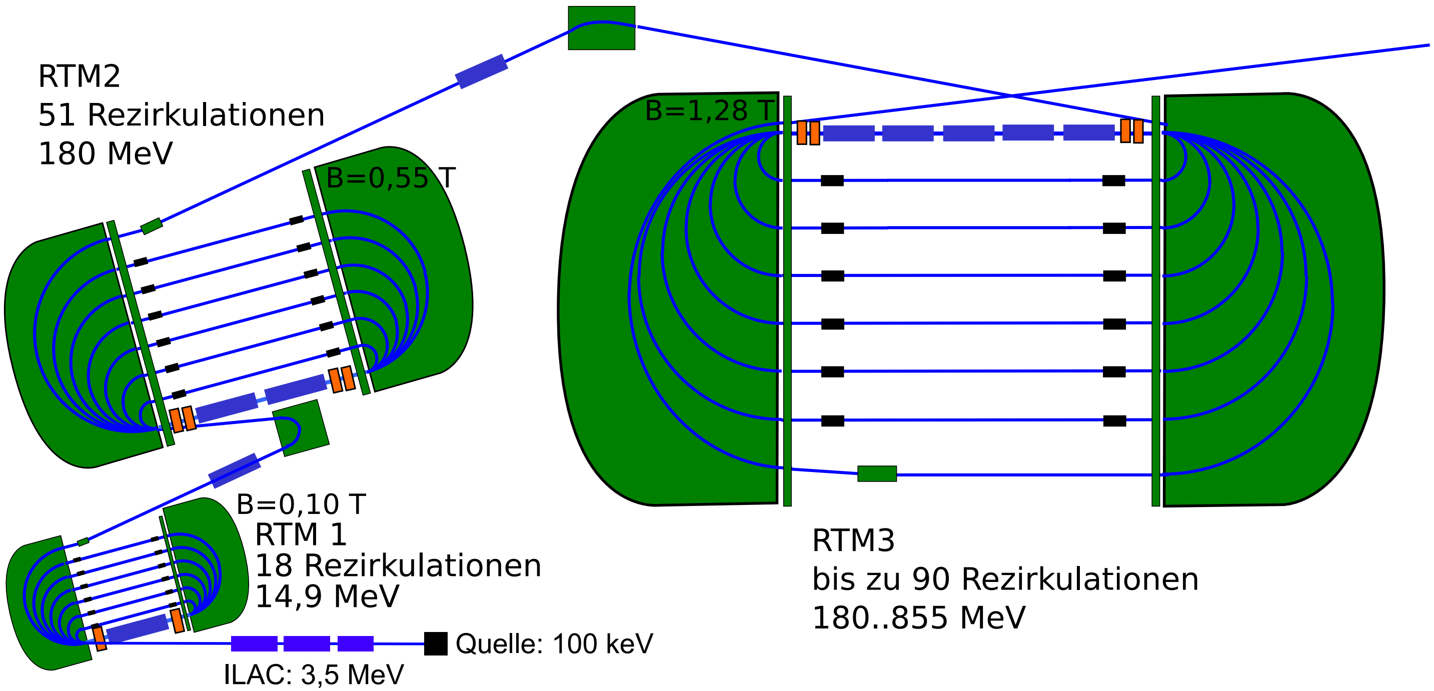

- source (thermal gun / polarized gun): 100 keV
- injector linac (ILAC): 3.5 MeV
- RaceTrack Microtrons:
  - RTM1: 14 MeV
  - RTM2: 180 MeV
  - RTM3: up to 855 MeV (steps of 7.5 MeV)

MAMI – principle of operation

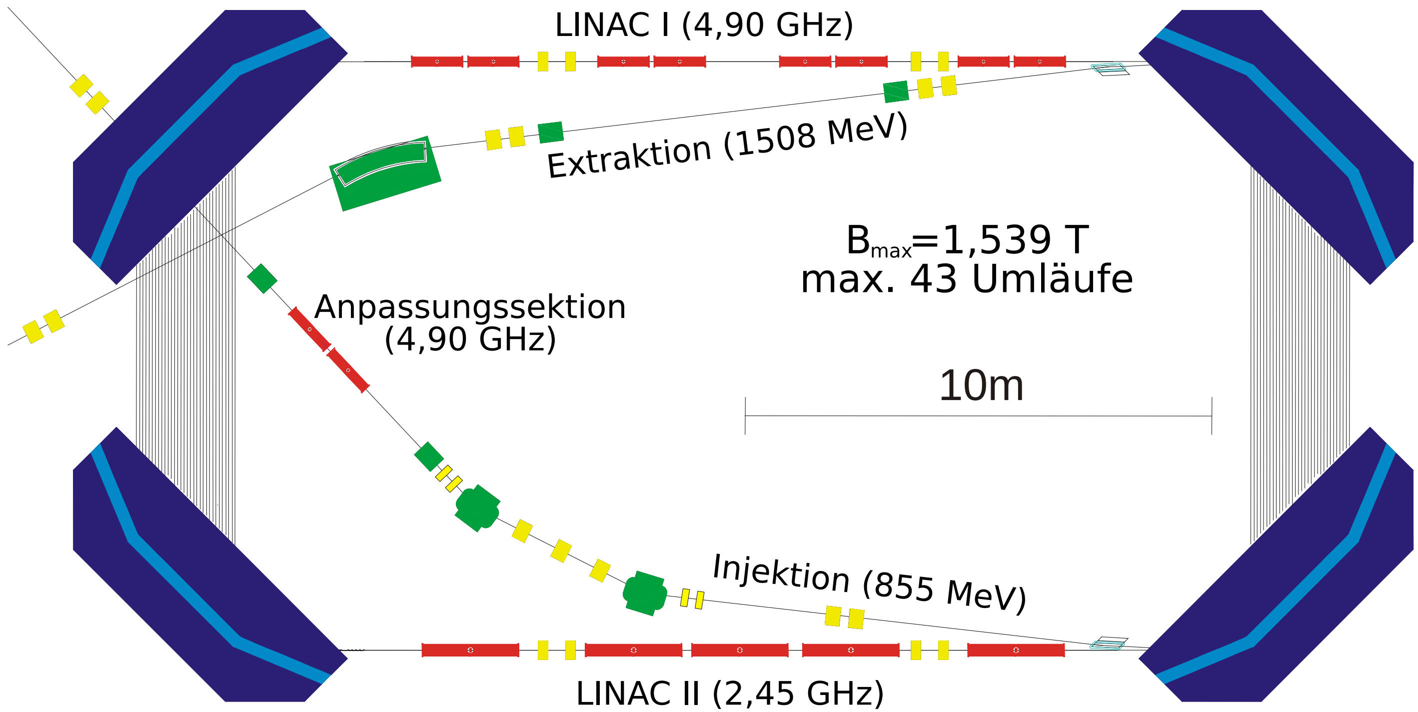

- Harmonic Double-Sided Microtron (HDSM):
  up to 1.5 GeV (1100..1508 in steps of 15 MeV)

MAMI – Groups at the Institute

Experiments

- B1 – Accelerator Operation & Development
- B2 – Polarized Source
- A1 – Electron Scattering
- A2 – Tagged Photons
- A4 – Parity Violation
- X1 – X-Rays

Theory

- χPT
- Lattice QCD (“Wilson”: 2240 CPU cores, 2.24 TB RAM, $\approx$17 TFlops (peak), 3.7 TF (sustained))

Parity Violation in Elastic Electron Scattering

Strangeness in the Proton

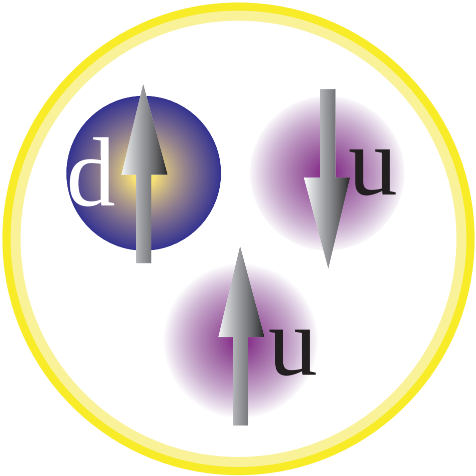

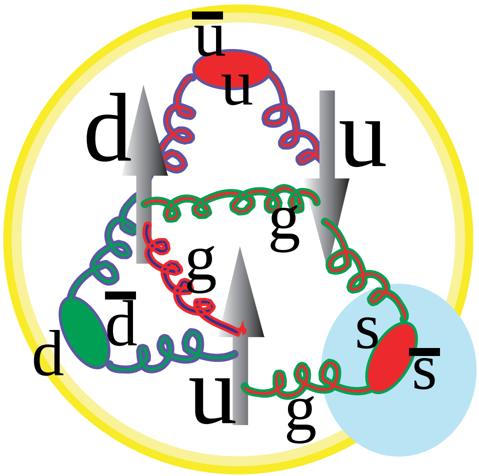

- sub-structure
- dynamical, strongly interacting system
- Access to the dynamical aspects of QCD:
  $\longrightarrow$ strangeness contributions to the vector formfactors
  $\longrightarrow$ parity violating electron scattering

Extraction of Strange Formfactors I

Hadronic current:

$$J^\mu = \sum_{f=u,d,s} Q_f \bar{f} \gamma^\mu f \qquad (1)$$

Parametrization using formfactors:

$$J^\mu = e\bar{u} \left(\sum_{f=u,d,s} q_f \left(F_1^f(Q^2)\gamma^\mu + \frac{1}{2M} F_2^f i\sigma^{\mu\nu} q_\nu \right) \right) u \qquad (2)$$

Dirac, Pauli $\longrightarrow$ Sachs formfactors:

$$\begin{aligned} G_E^{p,n}(Q^2) &= F_1^{p,n}(Q^2) - \tau F_2^{p,n}(Q^2) \\ G_M^{p,n}(Q^2) &= F_1^{p,n}(Q^2) - F_2^{p,n}(Q^2) \end{aligned} \qquad (3)$$

Extraction of Strange Formfactors II

Isospin symmetry & zero netto strangeness:

$$\begin{aligned} G^u_{E,M} &:= G^{p,u}_{E,M} = G^{n,d}_{E,M} \\ G^d_{E,M} &:= G^{p,d}_{E,M} = G^{n,u}_{E,M} \\ G^s_{E,M} &:= G^{p,s}_{E,M} = G^{n,s}_{E,M} \end{aligned} \quad (4)$$

Proton:

$$G^p_{E,M} = \frac{2}{3} G^u_{E,M} - \frac{1}{3} G^d_{E,M} - \frac{1}{3} G^s_{E,M} \quad (5)$$

Neutron:

$$G^n_{E,M} = \frac{2}{3} G^d_{E,M} - \frac{1}{3} G^u_{E,M} - \frac{1}{3} G^s_{E,M} \quad (6)$$

Extraction of Strange Formfactors III

Hadronic current with weak interaction:

$$\tilde{J}^{\mu} \sim \bar{u} \sum_{f=u,d,s} \left[q_V^f \left(\gamma^{\mu} \tilde{F}_1^f + i \frac{\tilde{F}_2^f}{2M} \sigma^{\mu\nu} q_{\nu} \right) - q_A^f \gamma^{\mu} \gamma^5 \tilde{G}_A^f \right] u \quad (7)$$

Quark *distributions* should not depend on type of interaction:

$$F_{1,2}^f = \tilde{F}_{1,2}^f \quad (8)$$

Therefore:

$$\tilde{G}_{E,M}^p = q_V^u G_{E,M}^u + q_V^d G_{E,M}^d + q_V^s G_{E,M}^s \quad (9)$$

This makes *two* relations, together with *four* relations from isospin symmetry for *six* vector formfactors $G_{E,M}^f$ to extract the *strange vector formfactors*.

The A4 experiment

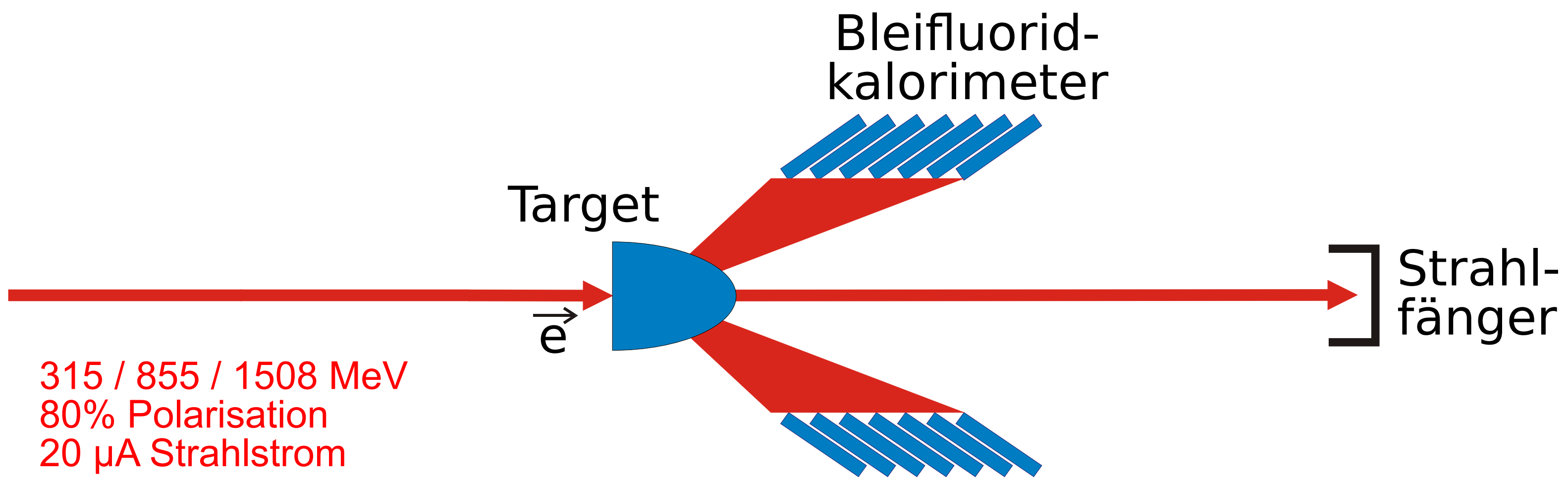

$$A_{PV} = \frac{\sigma^+ - \sigma^-}{\sigma^+ + \sigma^-} = A_0 + A_S$$

$$A_S = \frac{A_{exp}}{P_e} - A_0$$

The A4 experiment

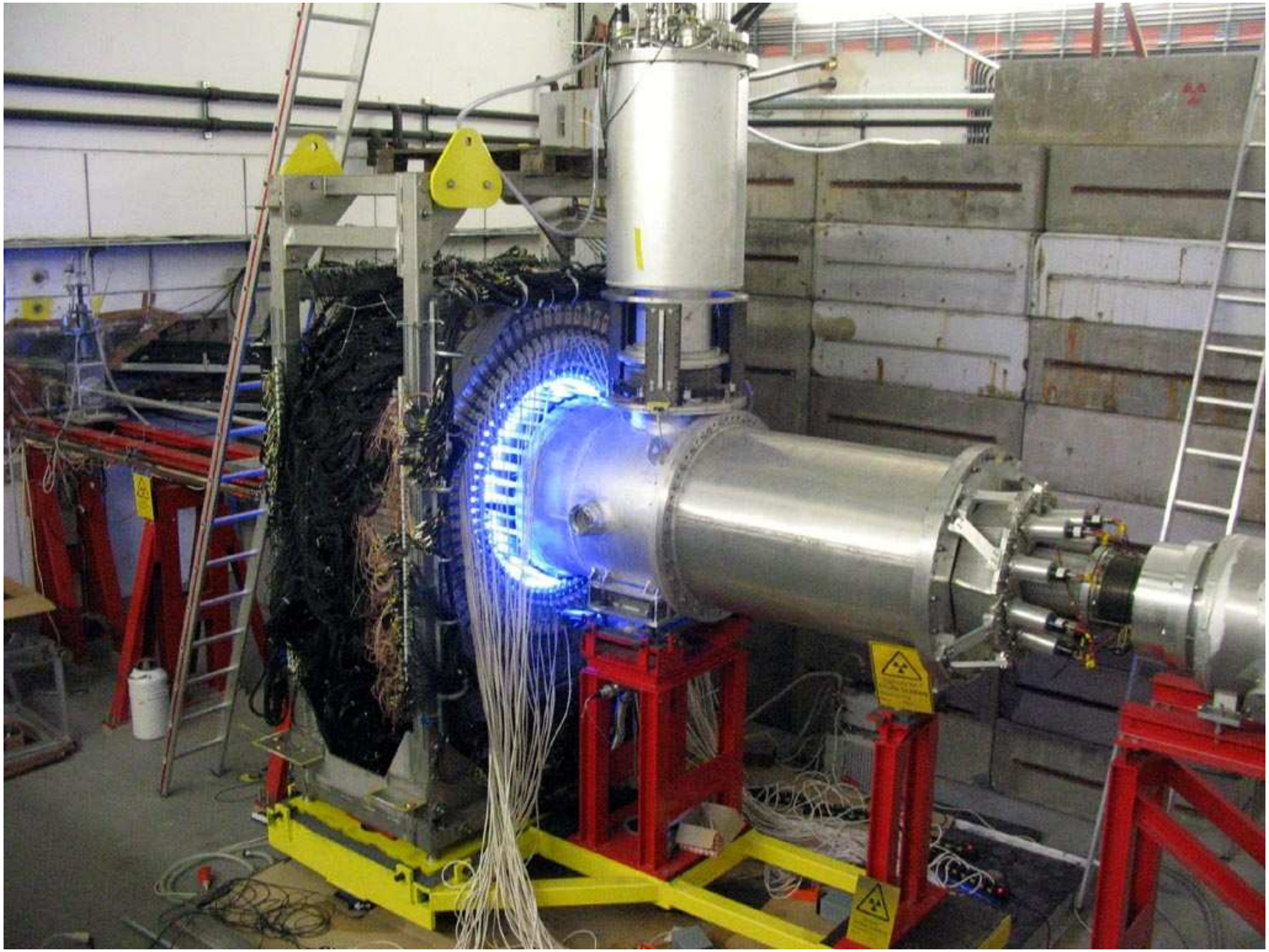

The A4 experiment

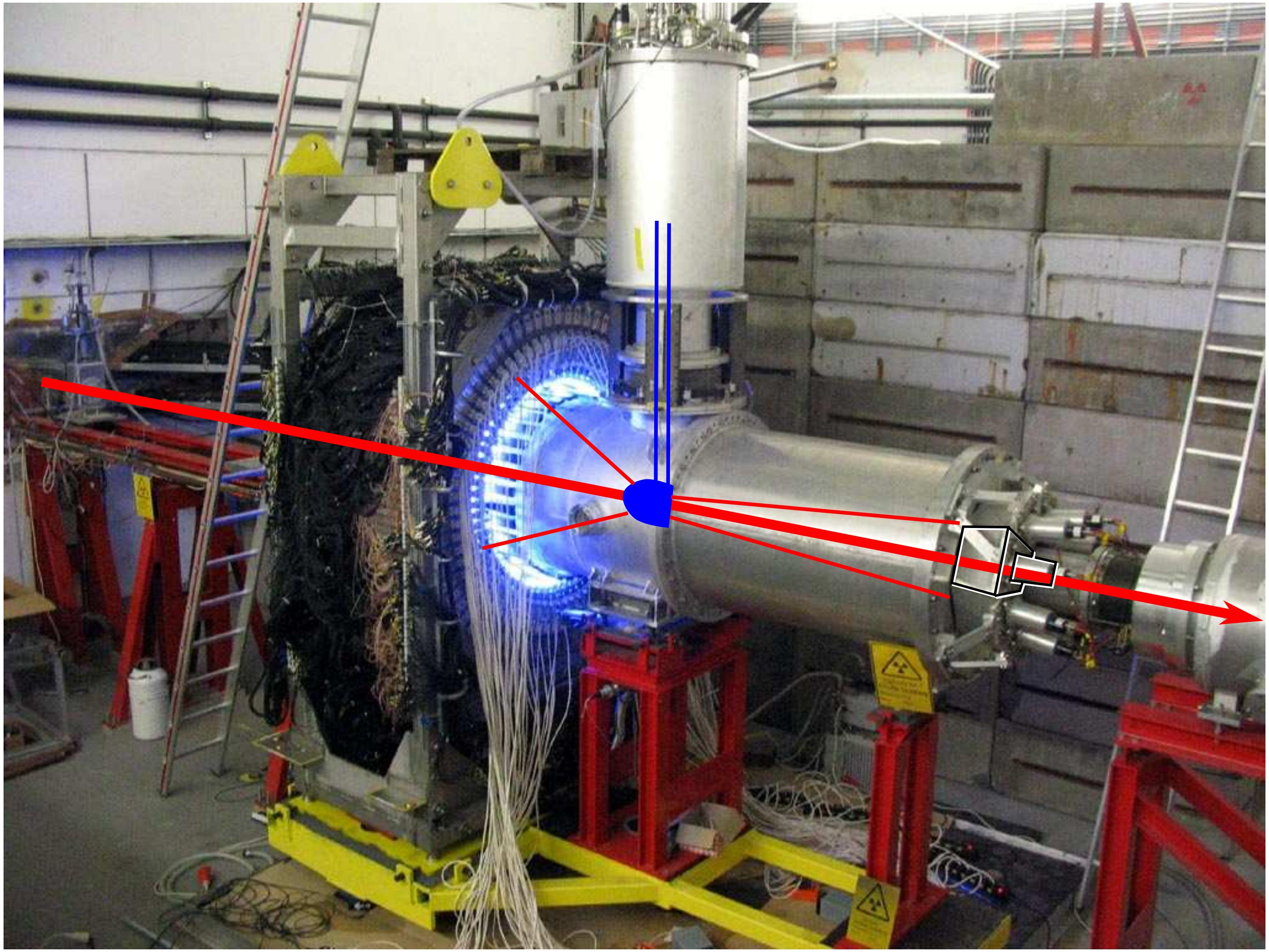

The A4 experiment

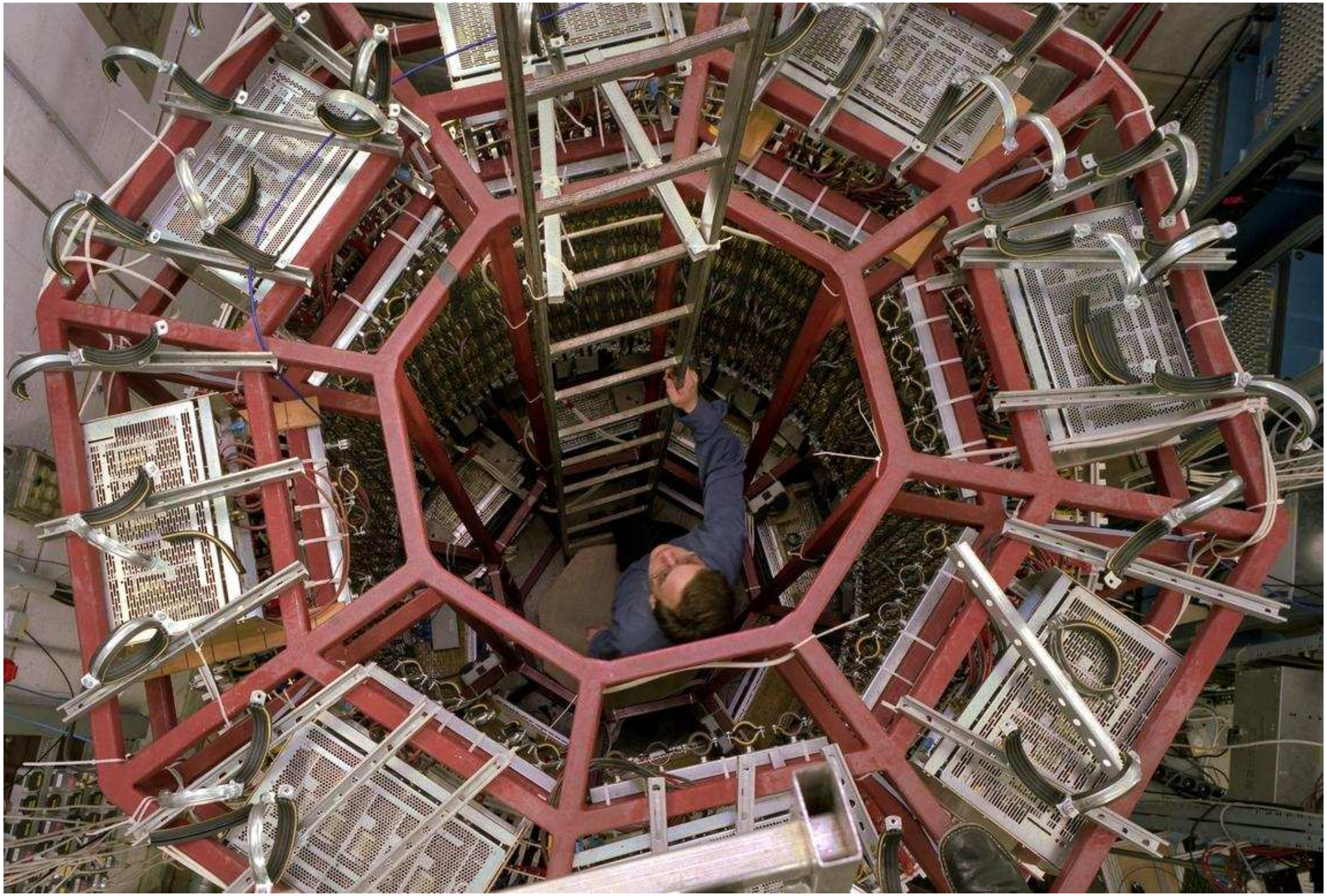

The A4 experiment

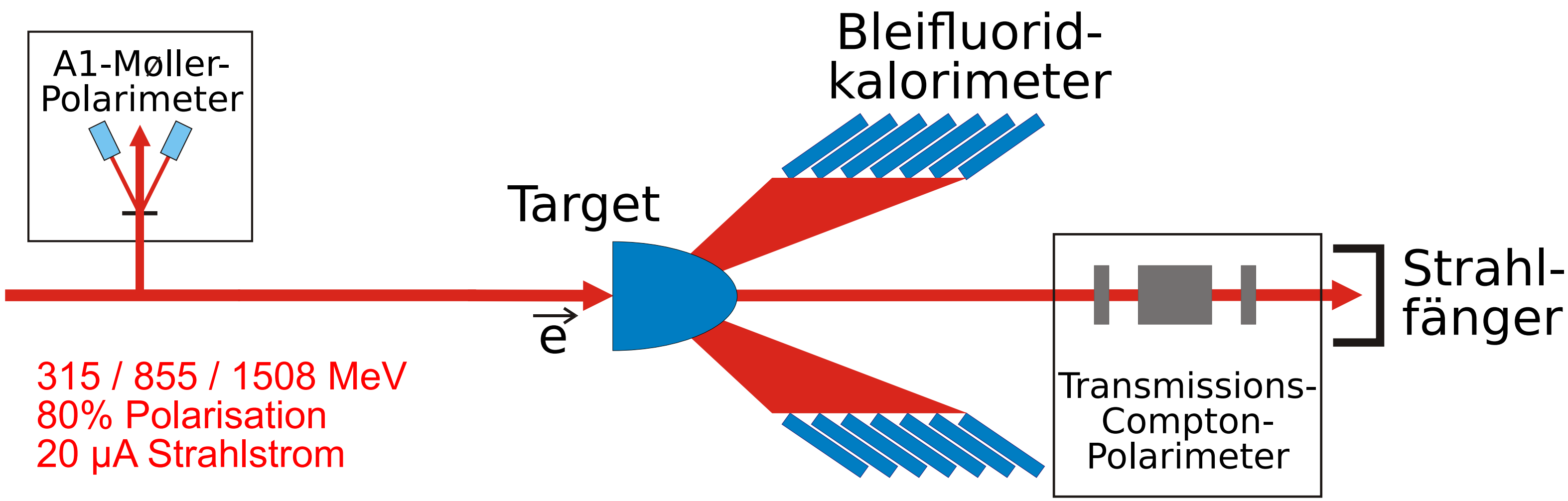

$$A_{PV} = \frac{\sigma^+ - \sigma^-}{\sigma^+ + \sigma^-} = A_0 + A_S$$

$$A_S = \frac{A_{exp}}{P_e} - A_0$$

so far: $\Delta P_e / P_e = 5\ \%$

The A4 experiment

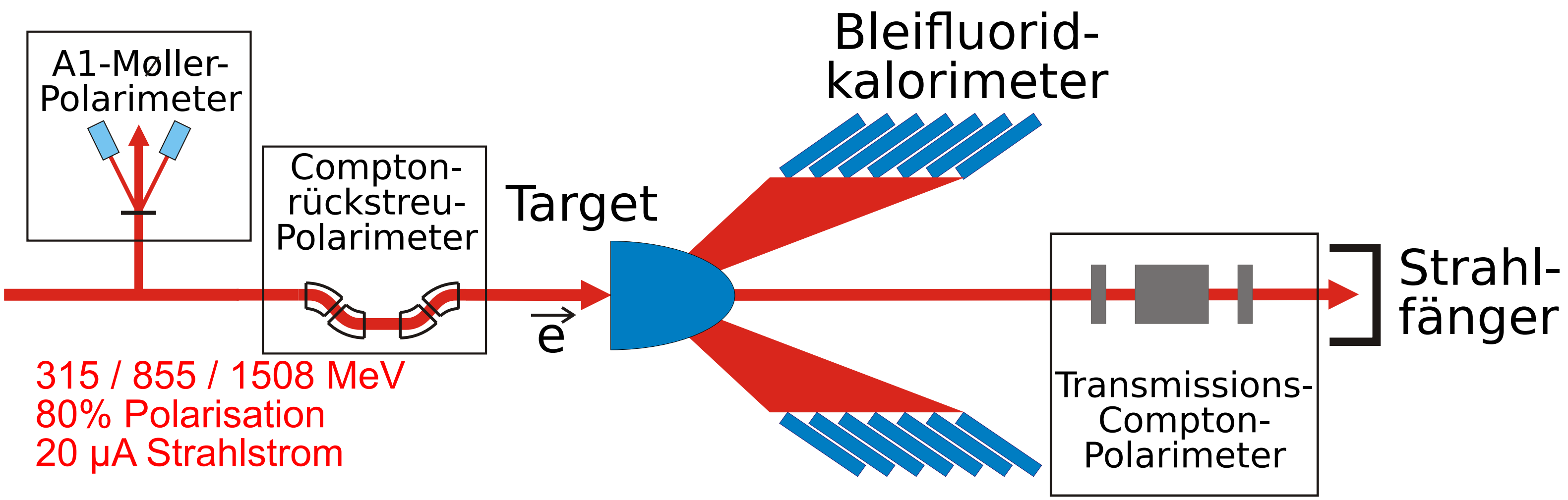

$$A_{PV} = \frac{\sigma^+ - \sigma^-}{\sigma^+ + \sigma^-} = A_0 + A_S$$

$$A_S = \frac{A_{exp}}{P_e} - A_0$$

Goal: $\Delta P_e / P_e \approx 1\,\%$

Interpolation of Polarization

Transmission Compton Polarimeter

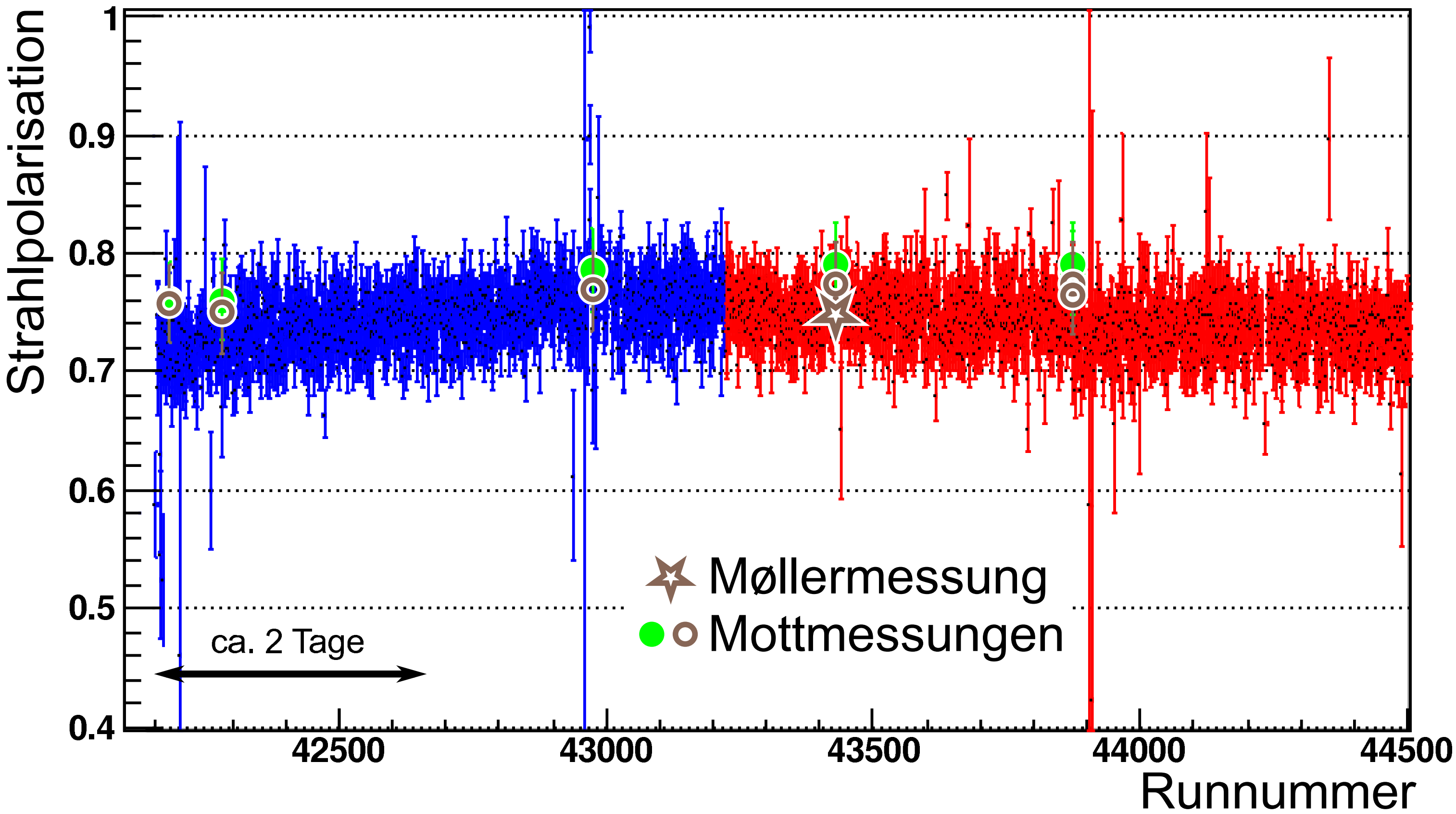

accuracy 1 % in 30 minutes

absolute calibration with the A1 Møller Polarimeter

Polarimeters at MAMI

A1 Møller Polarimeter

- absolute
- 1 % in 4 hours
- destructive
- A1 beam line
  $\longrightarrow$ systematics
  $\longrightarrow$ time consuming

B2 Mott Polarimeter

- relative (absolute)
- 1 % in 10 minutes
- destructive

A4 Transmission Compton Polarimeter

- relative
- non-destructive (behind target)
- 1 % in 30 minutes

Polarimeters at MAMI

A1 Møller Polarimeter

- absolute
- 1 % in 4 hours
- destructive
- A1 beam line
  $\longrightarrow$ systematics
  $\longrightarrow$ time consuming

B2 Mott Polarimeter

- relative (absolute)
- 1 % in 10 minutes
- destructive

A4 Transmission Compton Polarimeter

- relative
- non-destructive (behind target)
- 1 % in 30 minutes

A4 Compton Backscattering Polarimeter

- **absolute**
- **non-destructive**
- 1 % in 24/48 h (1508/855 MeV)
- **in front of target!**

Compton Polarimetry

Principle of Compton Polarimetry

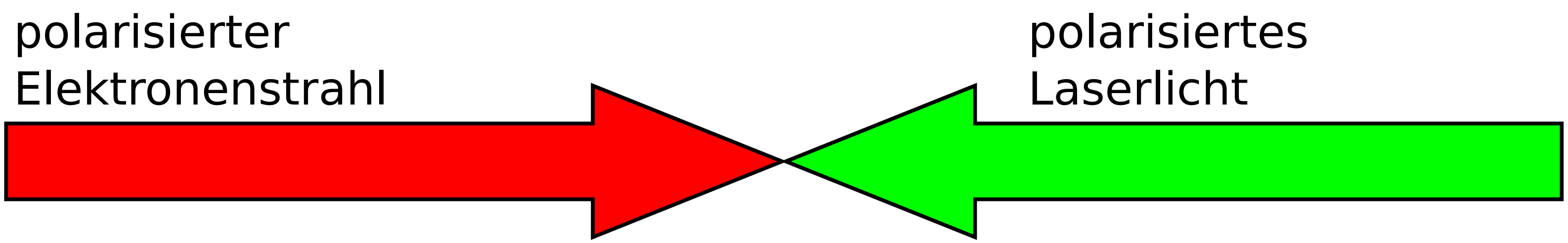

Principle of Compton Polarimetry

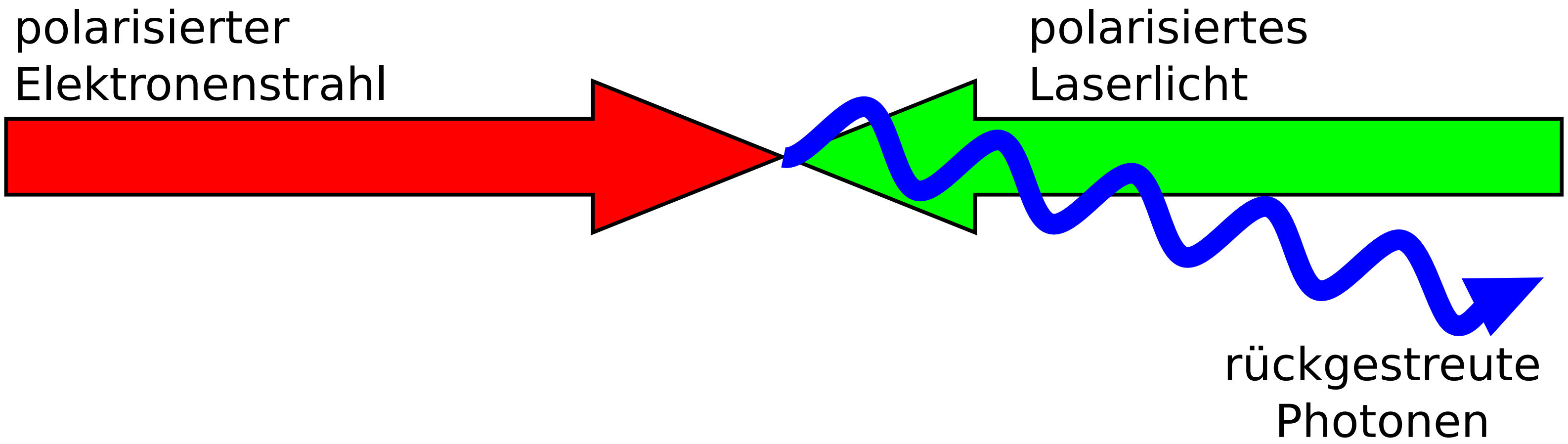

Principle of Compton Polarimetry

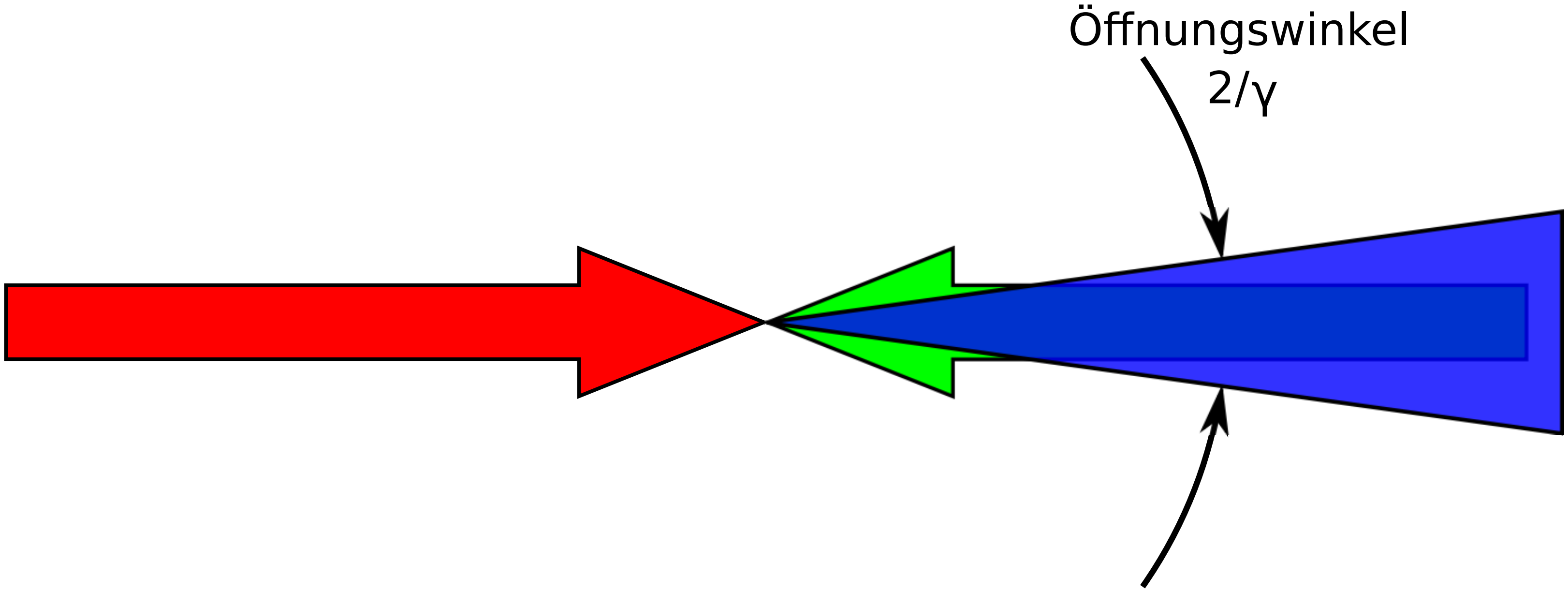

Cross Section

$$\frac{d\sigma}{d\rho} = \frac{d\sigma_0}{d\rho} - P_e P_L \frac{d\sigma_p}{d\rho} \quad \text{where} \quad \rho = k_f / k_f^{max}$$

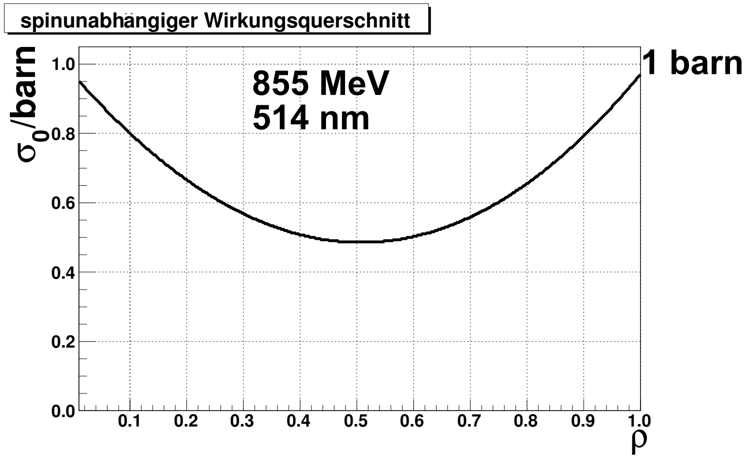

spin-independent part σ_0

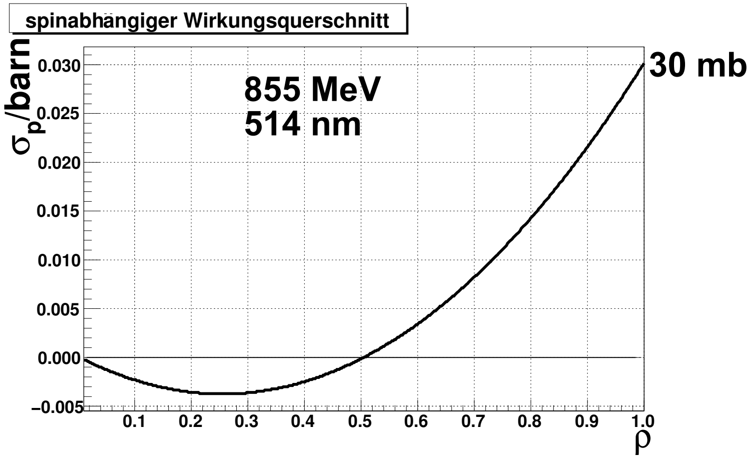

spin-dependent part σ_p

Cross Section

$$\frac{d\sigma}{d\rho} = \frac{d\sigma_0}{d\rho} - P_e P_L \frac{d\sigma_p}{d\rho} \quad \text{where} \quad \rho = k_f / k_f^{max}$$

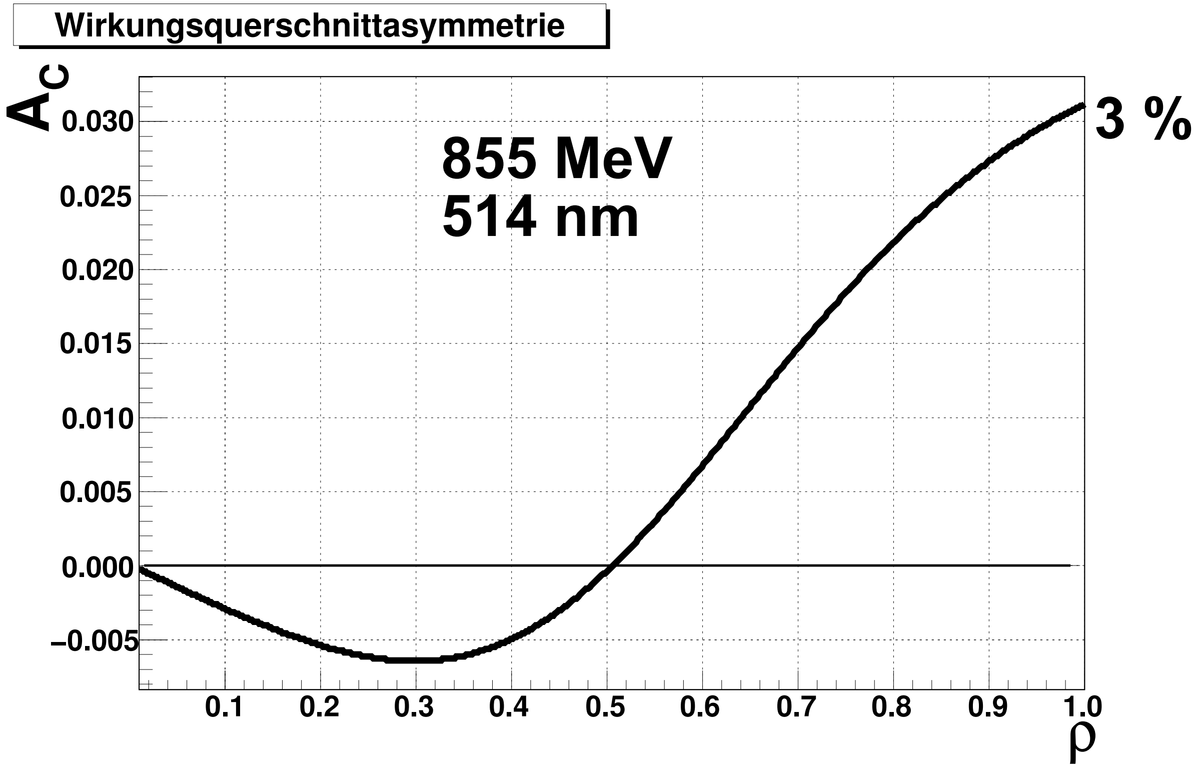

Compton asymmetry A_C

Experimental Realization

The A4 Compton Polarimeter

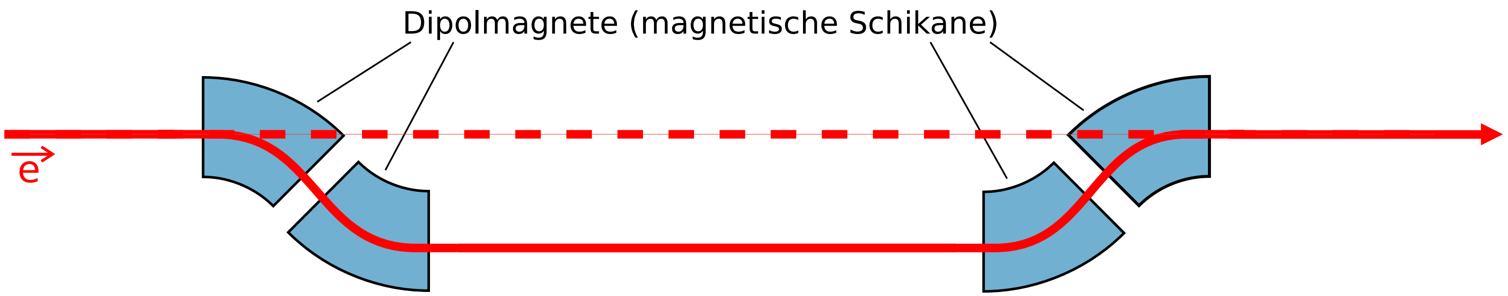

The A4 Compton Polarimeter

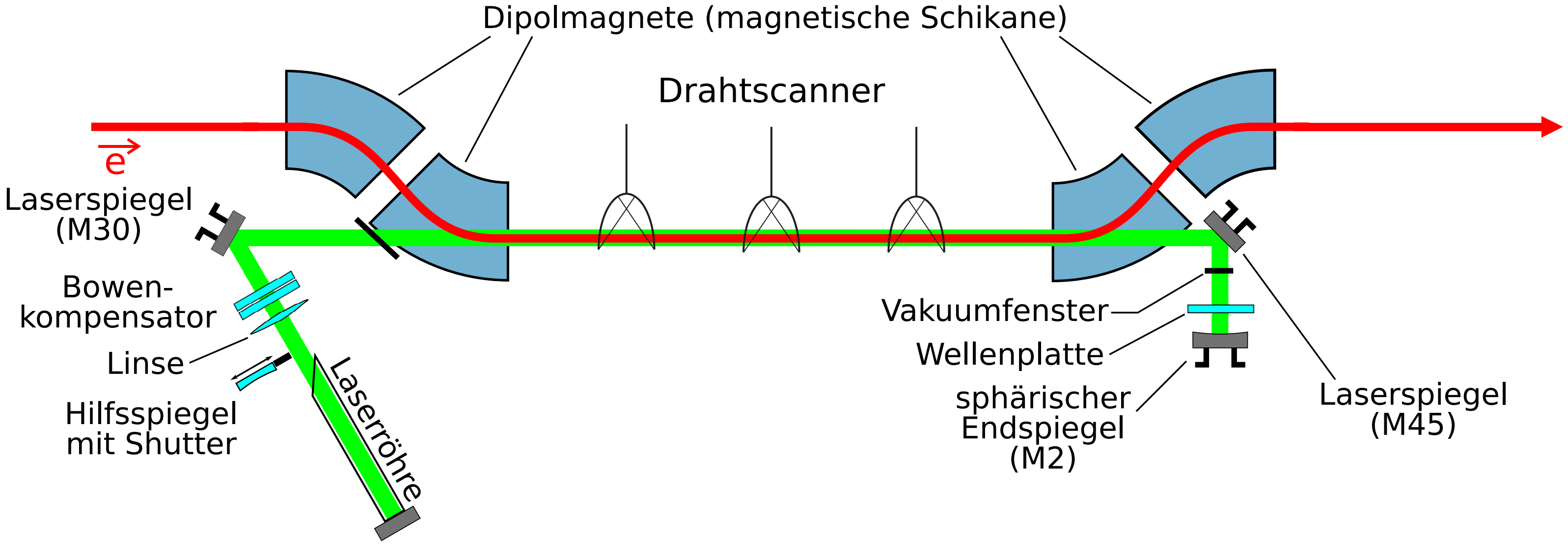

The A4 Compton Polarimeter

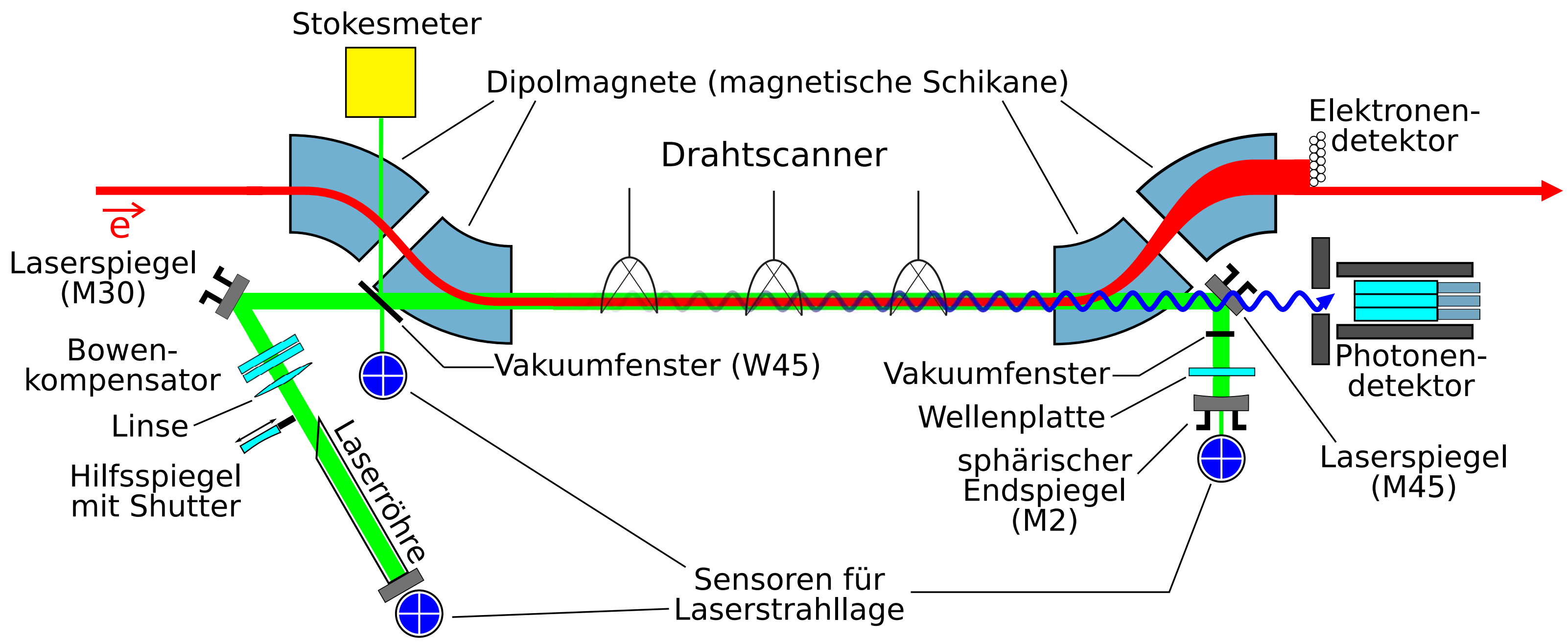

The A4 Compton Polarimeter

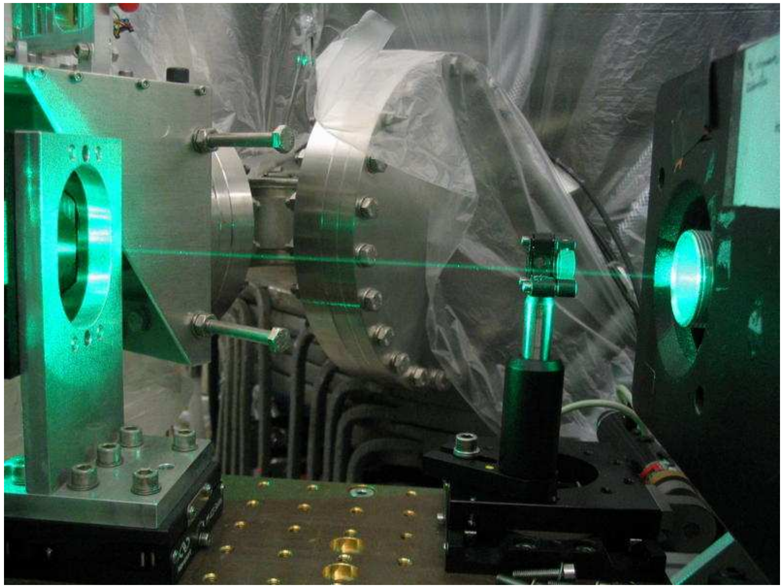

Detectors

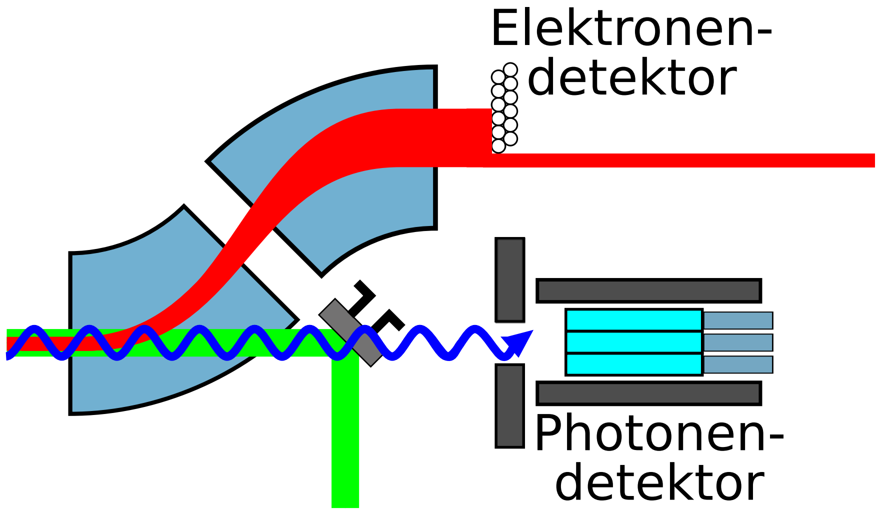

- photon calorimeter (energy spectra)
- use second half of chicane as magnetic spectrometer
- electron detector
  $\longrightarrow$ momentum-resolved detection of electrons in coincidence with photons
  $\longrightarrow$ tagged photons

Detectors

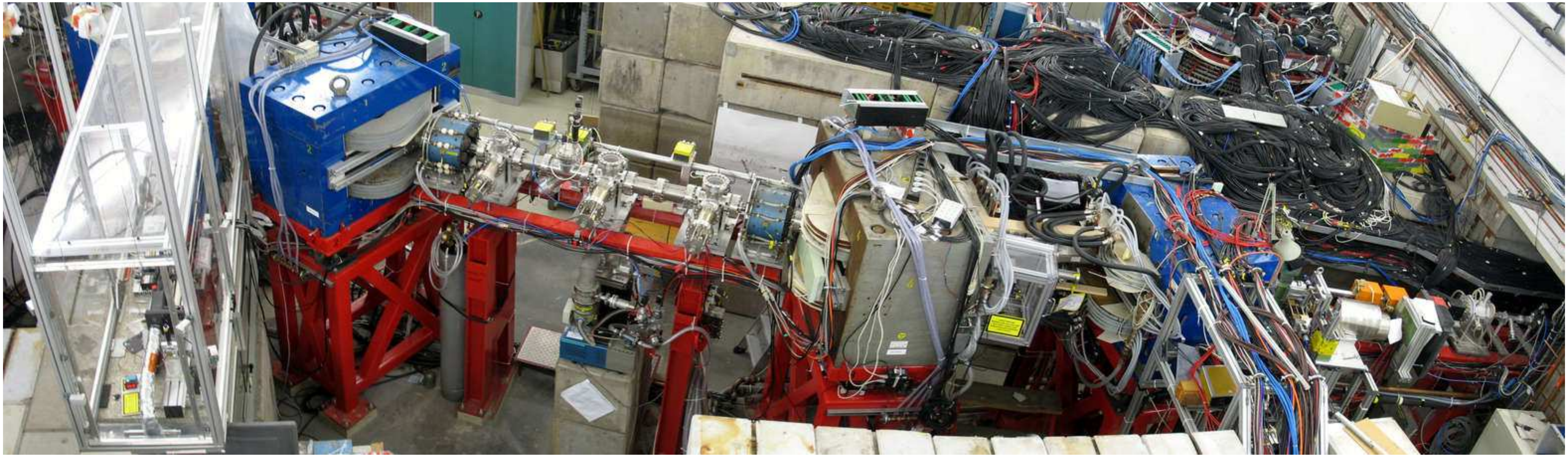

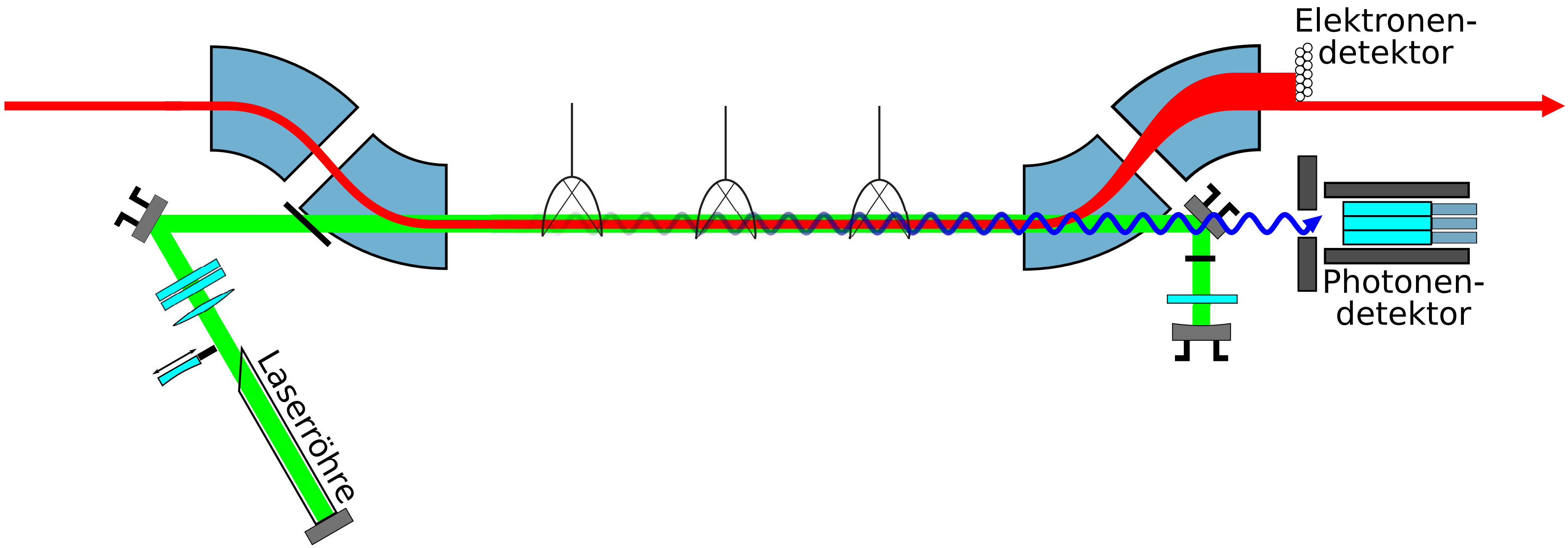

Detectors

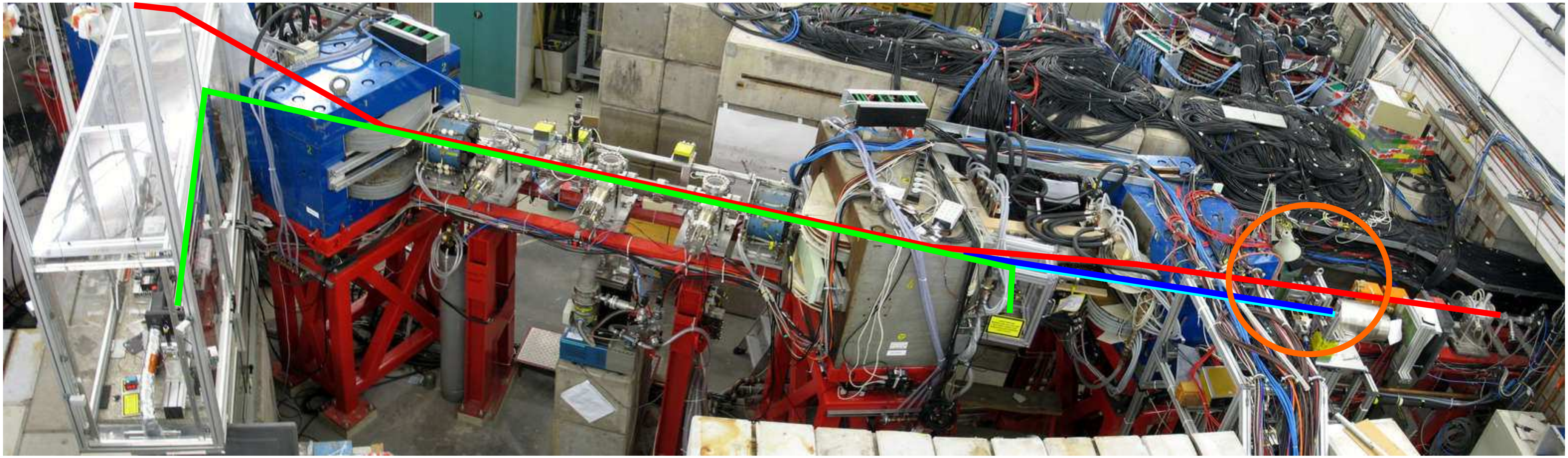

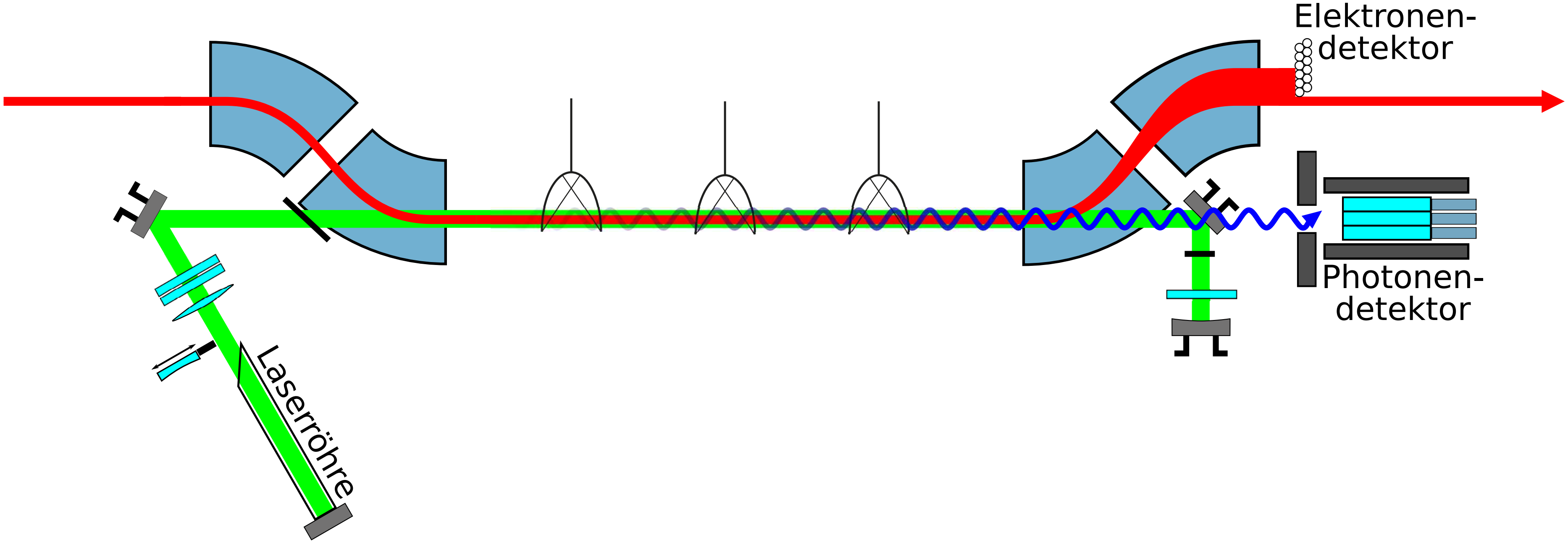

Detectors

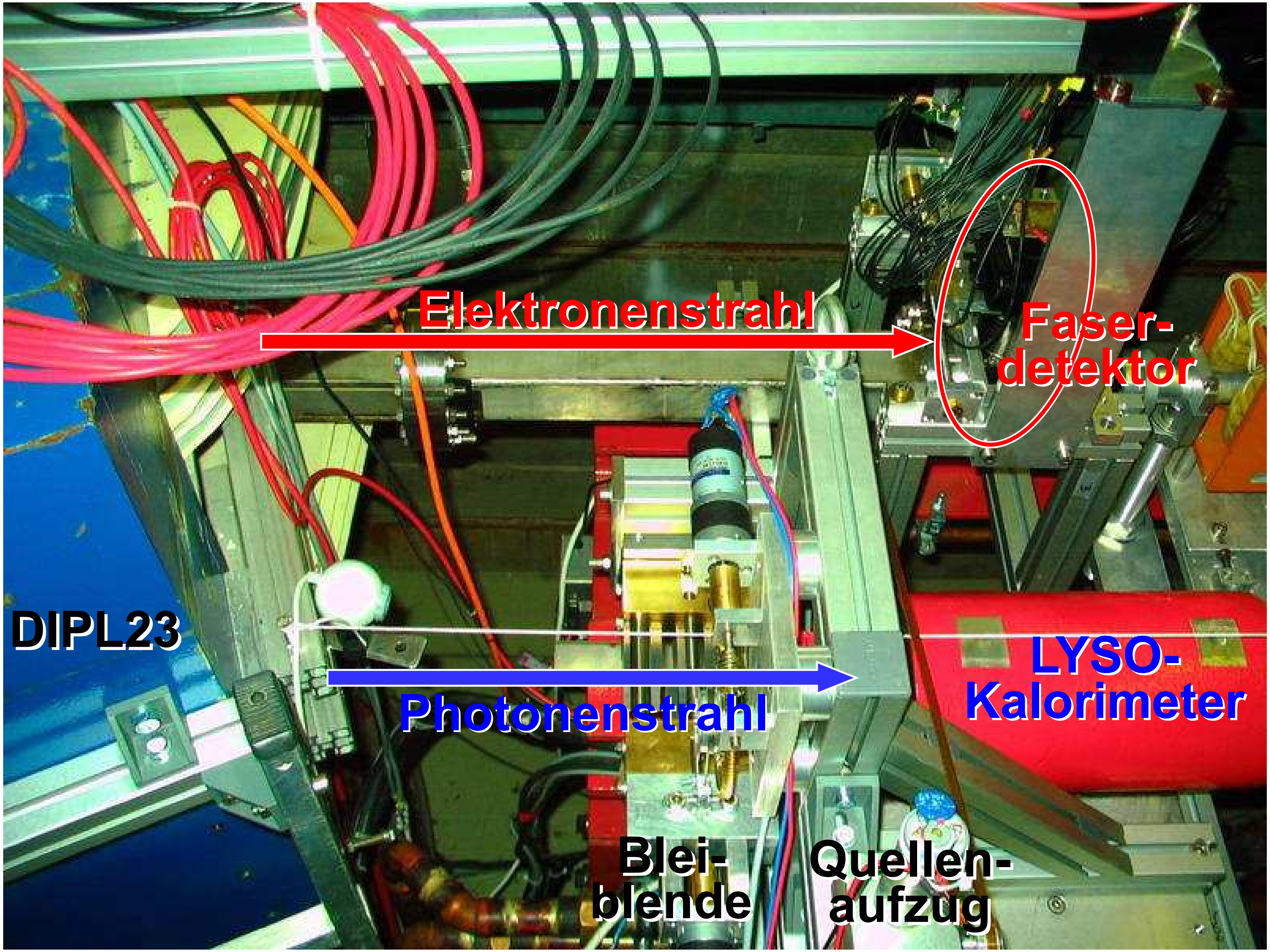

Elektronenstrahl
Faser-detektor
DIPL23
Photonenstrahl
LYSO-Kalorimeter
Blei-blende
Quellen-aufzug

Photon Detector

LYSO ($Lu_{1.8}Y_{0.2}SiO_5$),
PreLude420 from Saint Gobain

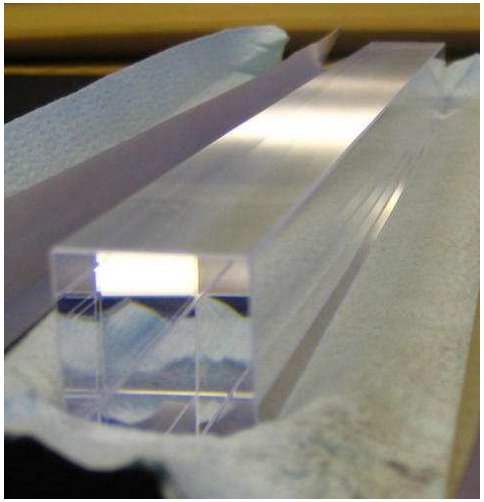

- density: 7.1 g/cm^3
- X_0: 12 mm
- τ: 41 ns
- light yield: 32 photons/keV, ≈75% of NaI(Tl)

crystals: 20x20x200 mm^3

3×3 crystals in DF2000MA (dielectr. reflective from 3M)

fast, compact calorimeter
for 1.5 ... 100 MeV photons

Electron Detector

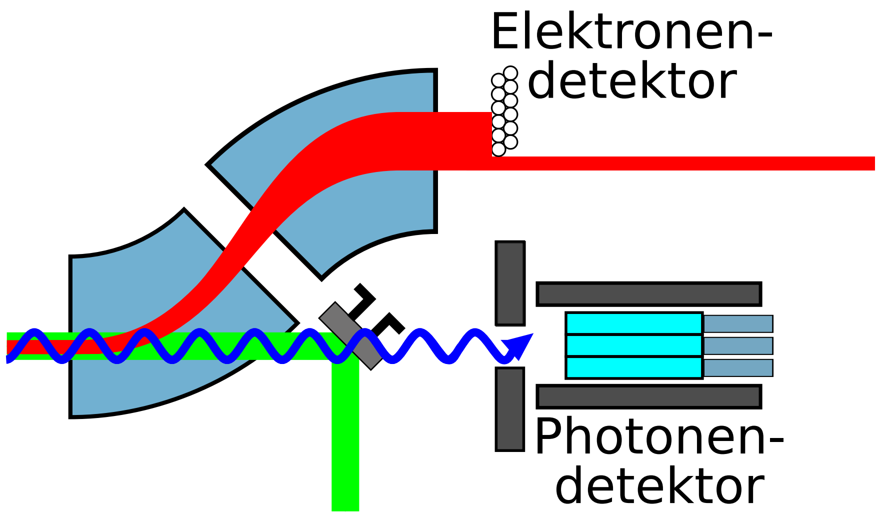

- 48 fibers
- 24 logic channels
- plastic scintillator
- photon tagger
- 0.78 mm resp. 1.9 MeV per fiber @ 855 MeV

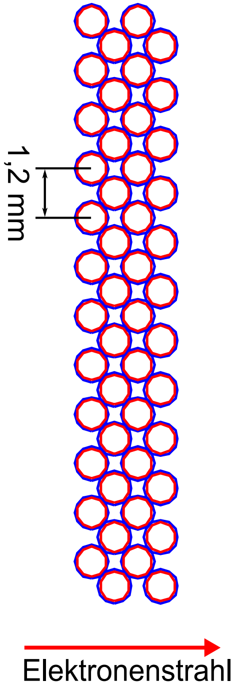

Electron Detector

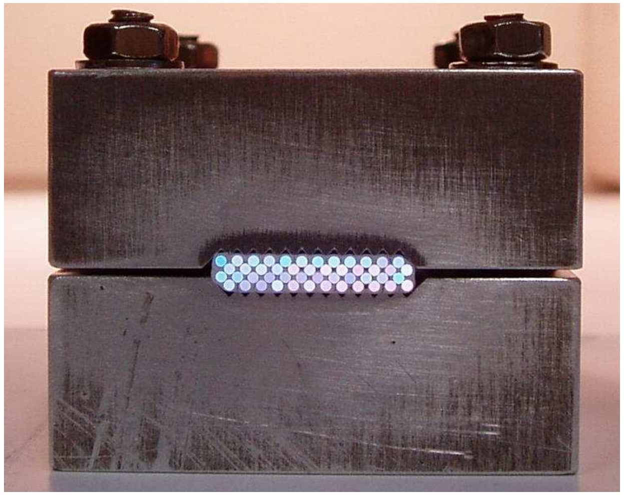

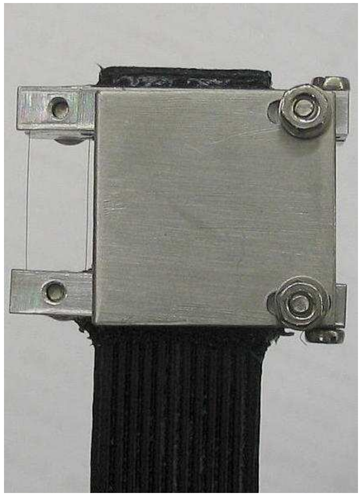

- 48 fibers
- 24 logic channels
- plastic scintillator
- photon tagger
- 0.78 mm resp. 1.9 MeV per fiber @ 855 MeV

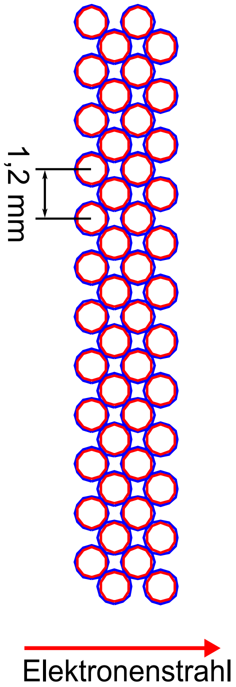

Data Acquisition

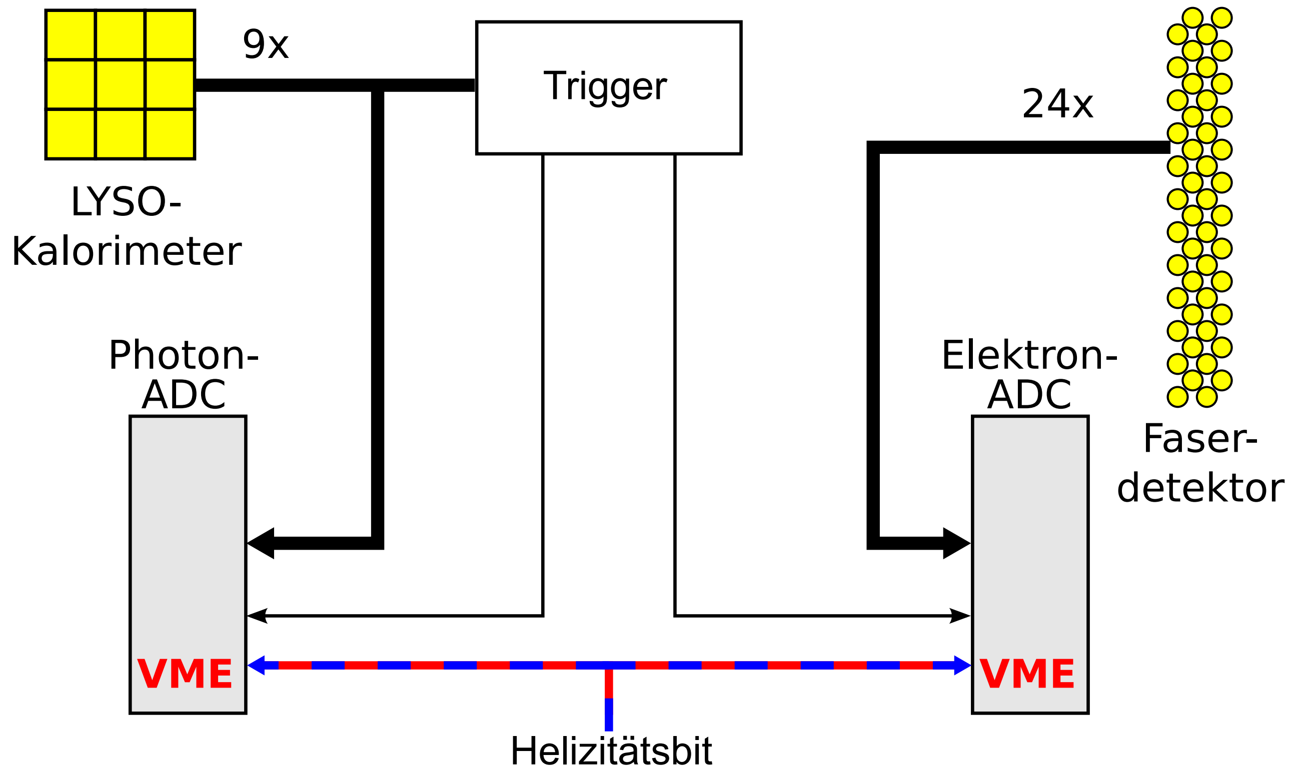

- trigger on every photon
- in addition: coincident + tagged photons
- max. readout rate approx. 60 kHz
- detector rates: helicity-correlated every 20 ms
- dedicated, symmetrical feed-in of helicity bit

Data Analysis

Background Subtraction

photon detector raw data

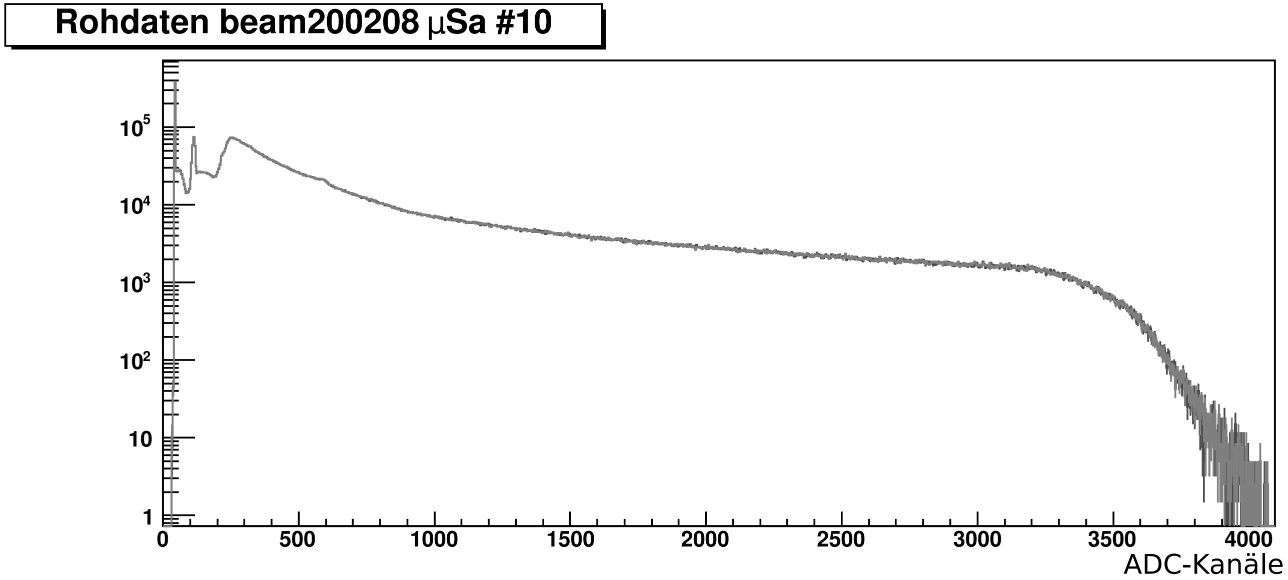

- gray: without laser light
- measurement w/o laser light to determine background

Background Subtraction

photon detector raw data

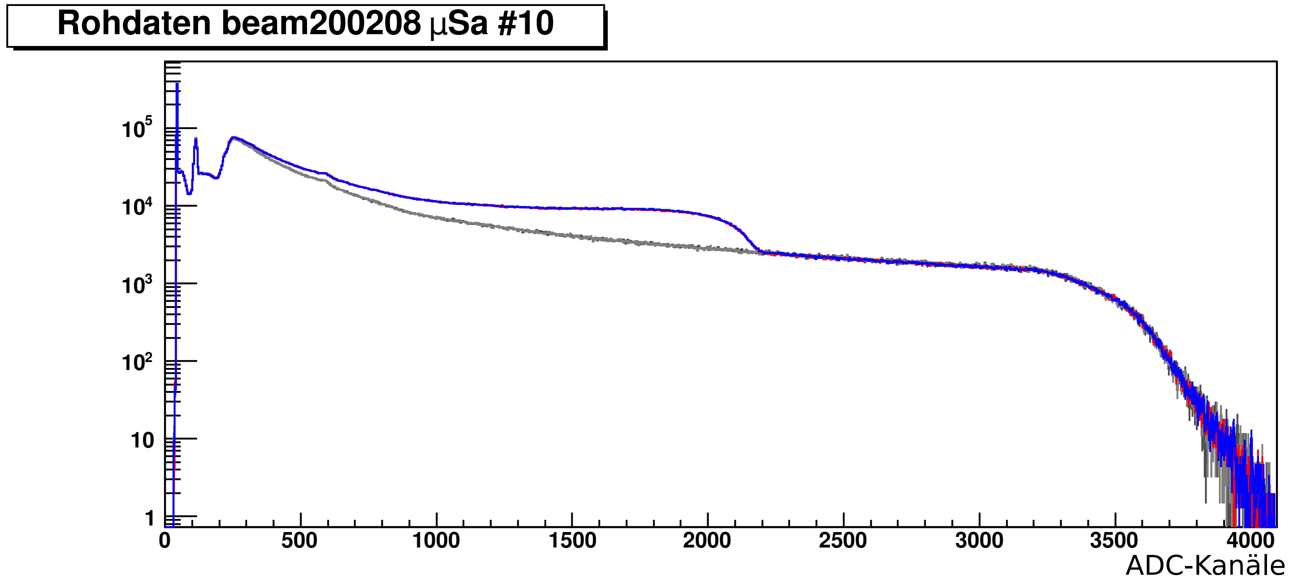

- red/blue: with laser light
- gray: without laser light
- measurement w/o laser light to determine background
- normalization above max. energy of backscattered photons

Background Subtraction

spectra of backscattered photons

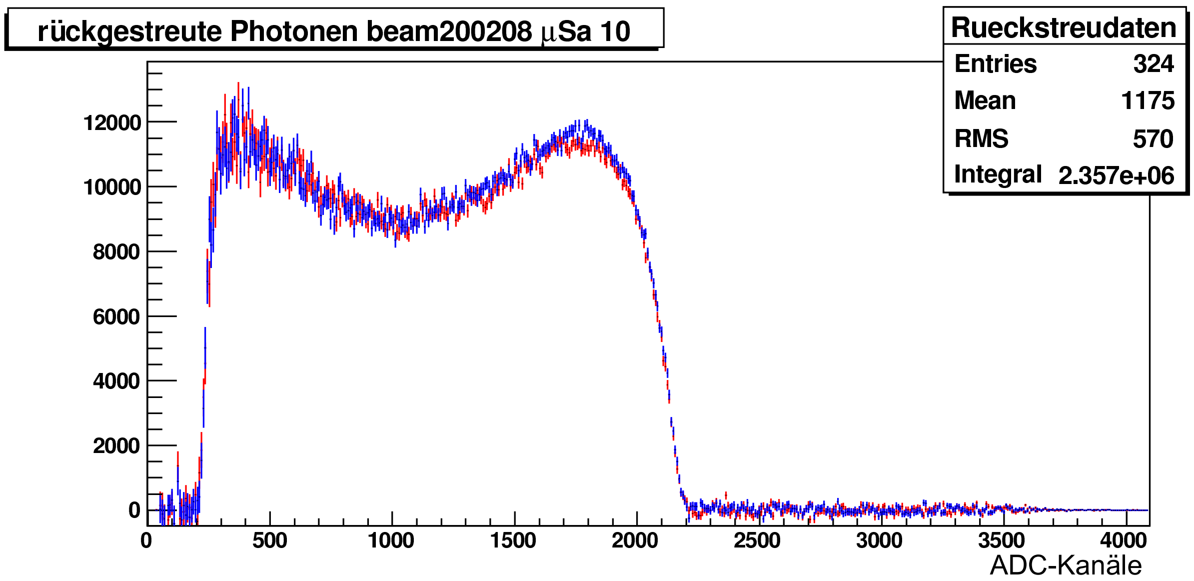

- after normalization and background subtraction
- red/blue: e^- beam helicity

Energy Calibration

absolute energy calibration

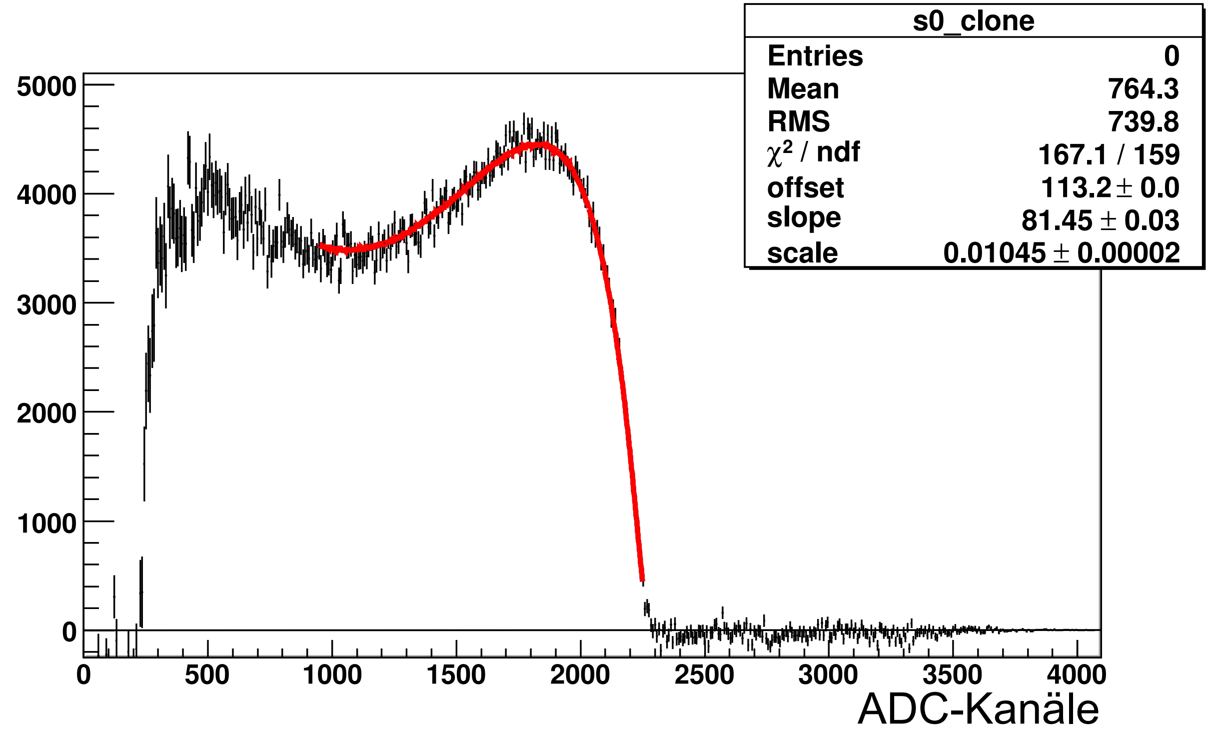

- fit simulated to measured backscattered photon spectrum
- parameters: pedestal und sensitivity (MeV/ch) of QDCs

Energy Calibration

absolute energy calibration

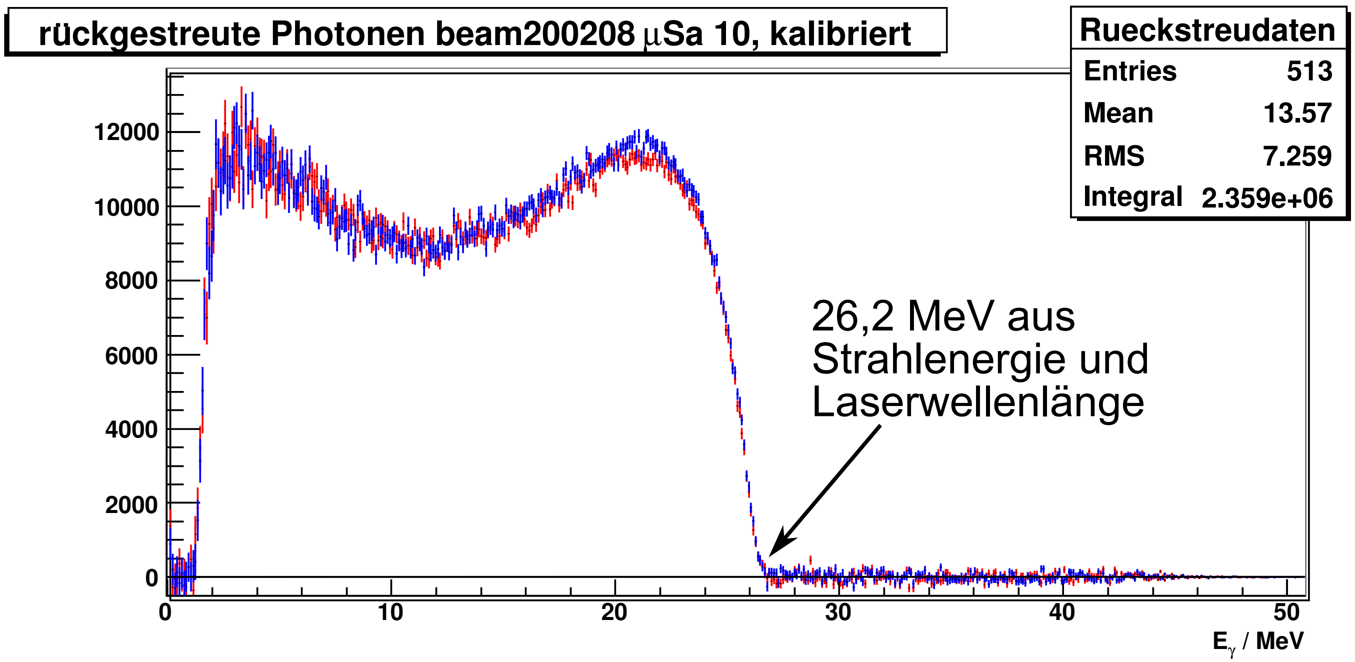

- fit simulated to measured backscattered photon spectrum
- parameters: pedestal und sensitivity (MeV/ch) of QDCs

Influence of Detector Response

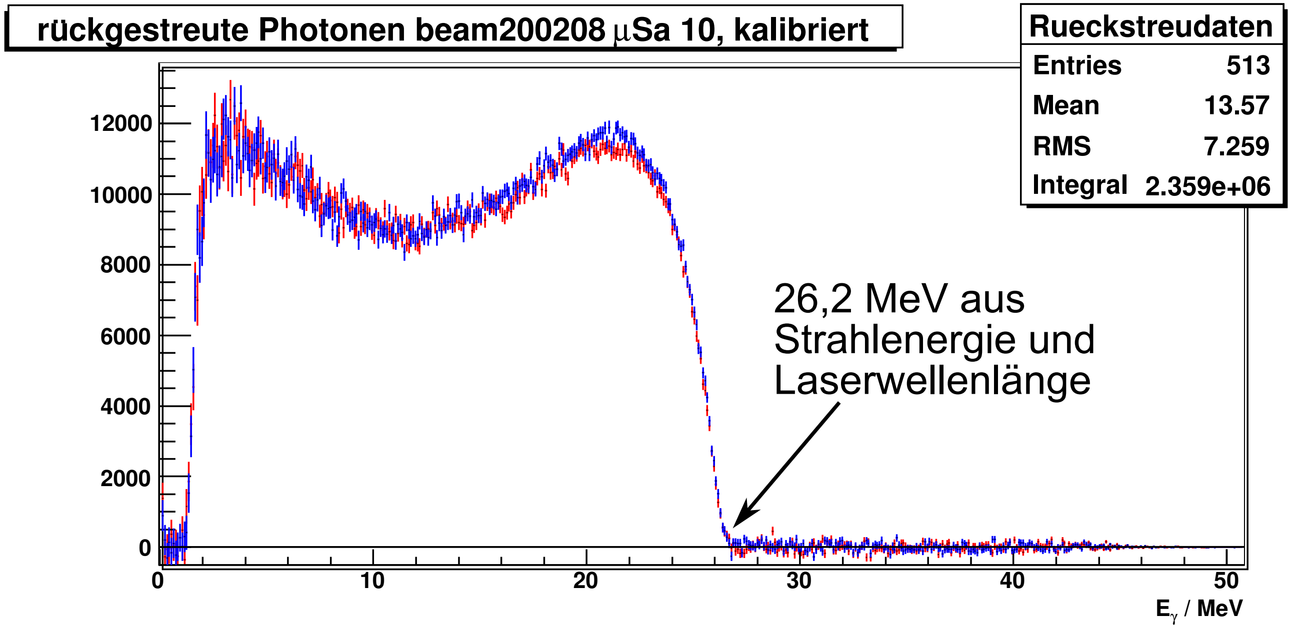

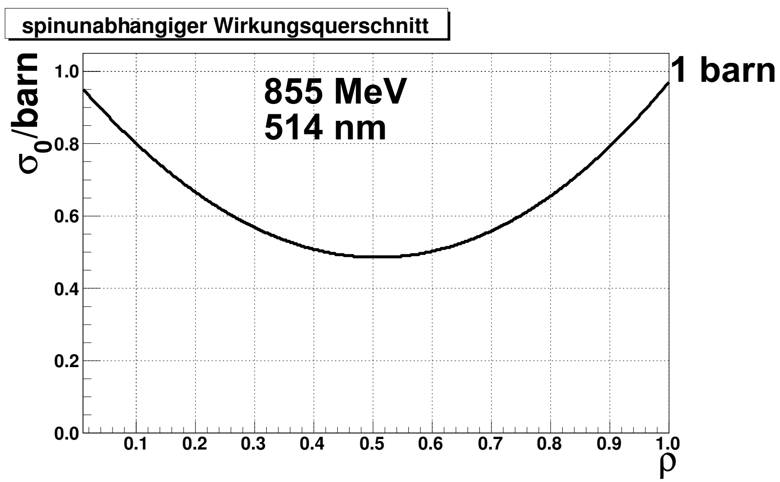

energy resolution, detector response...

Influence of Detector Response

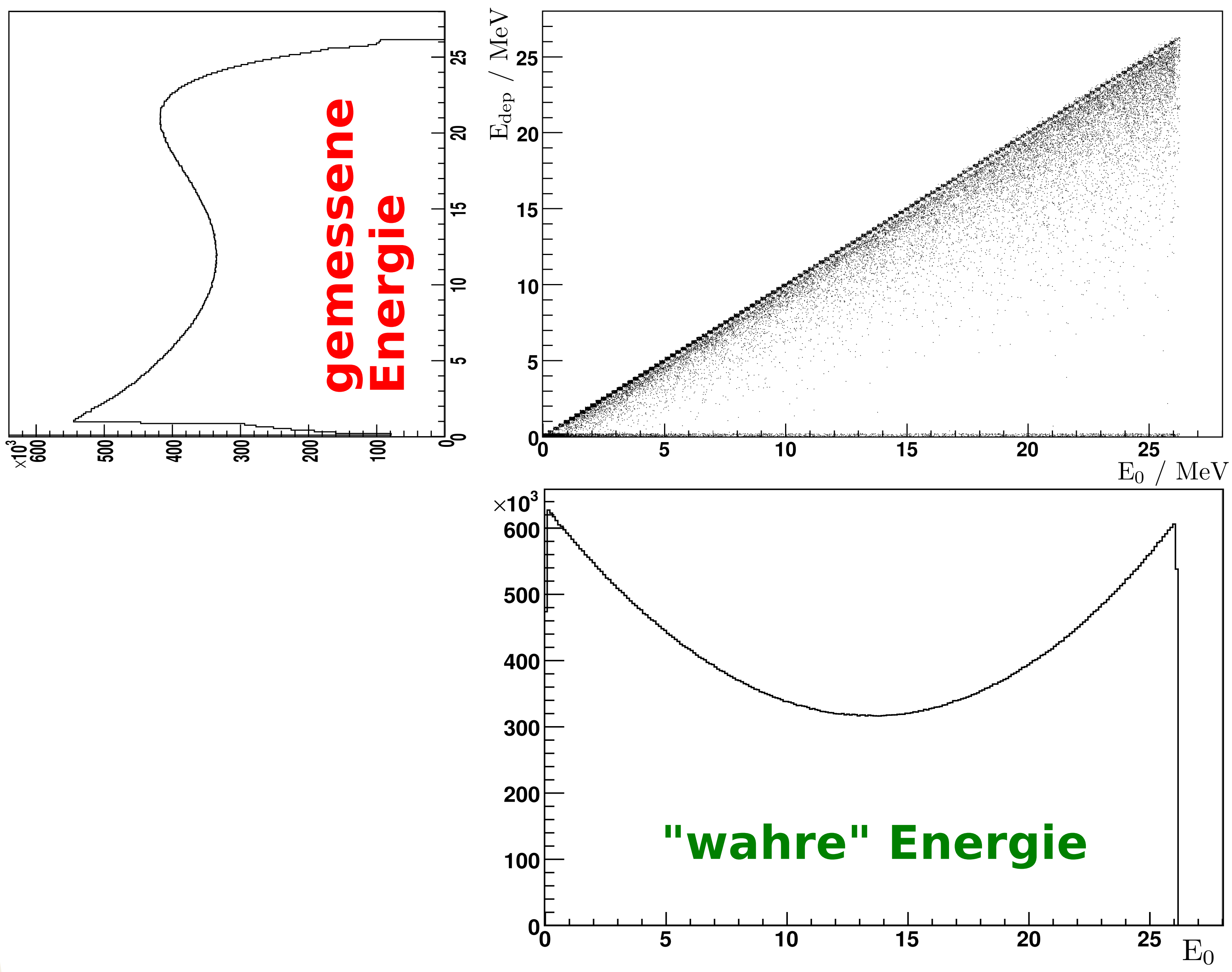

Raw Asymmetries

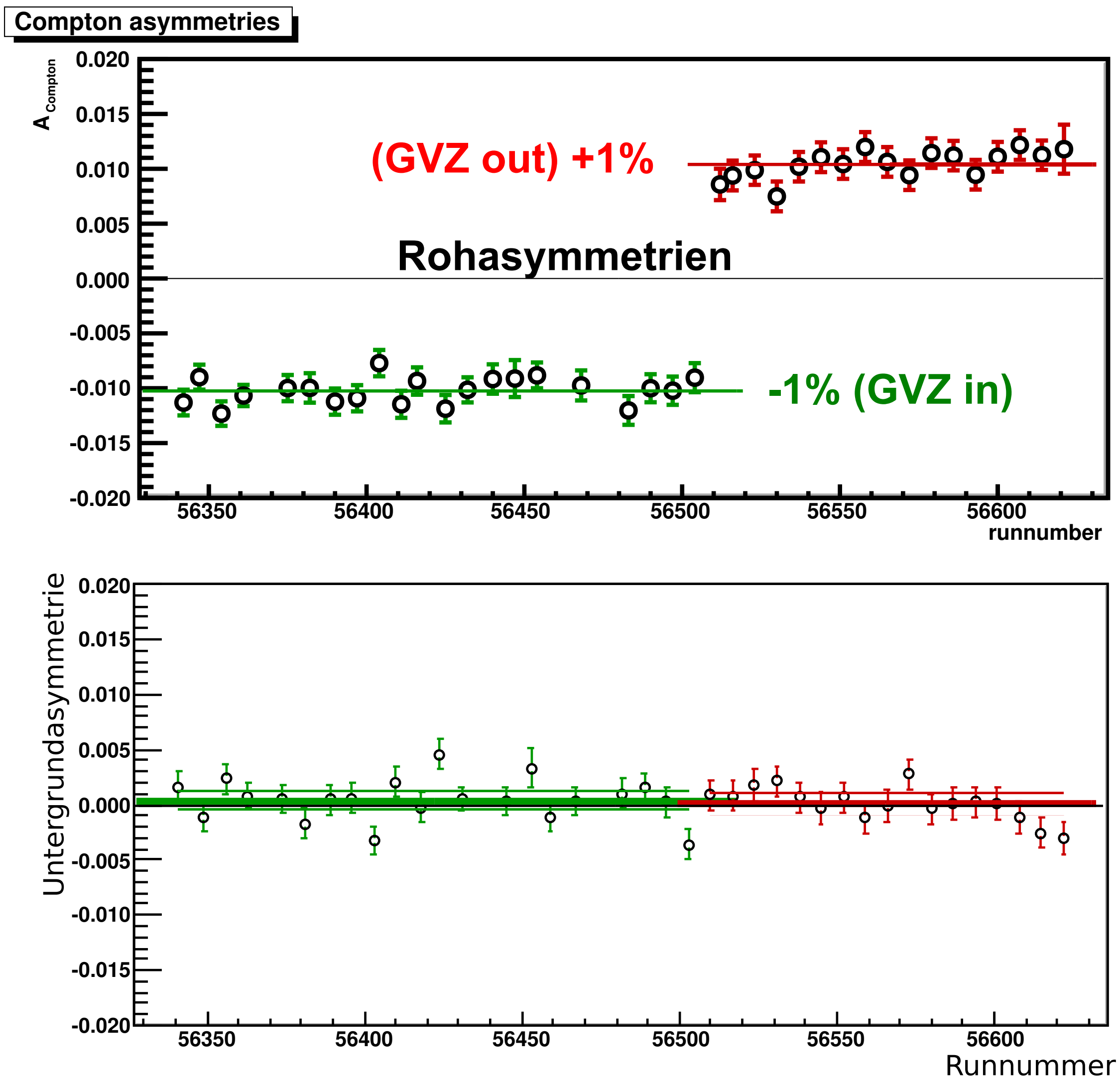

raw asymmetries, full spectra at 855 MeV

Determination of the Analyzing Power

- energy spectrum: cuts on *measured* energy
- required: cuts on *true* energy

Determination of the Analyzing Power

- energy spectrum: cuts on *measured* energy
- required: cuts on *true* energy

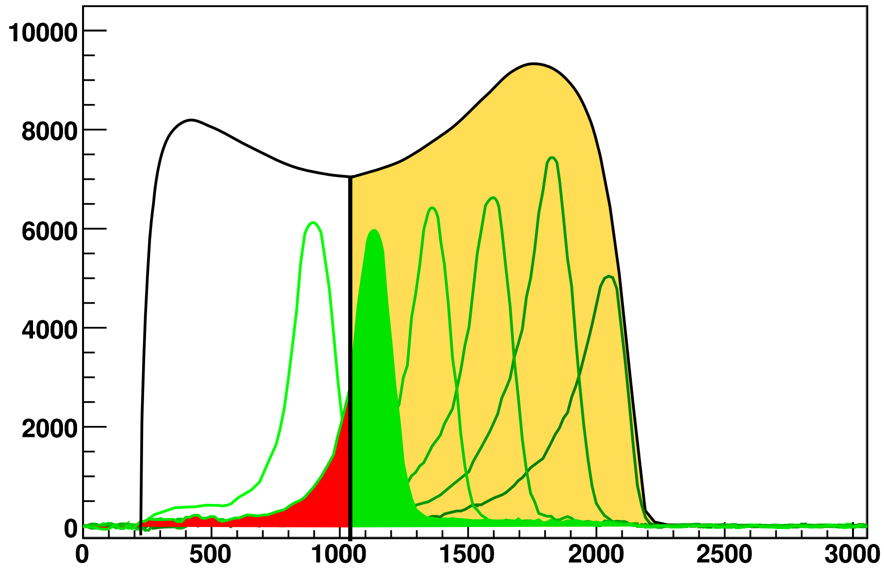

Determination of the Analyzing Power

- energy spectrum: cuts on *measured* energy
- required: cuts on *true* energy

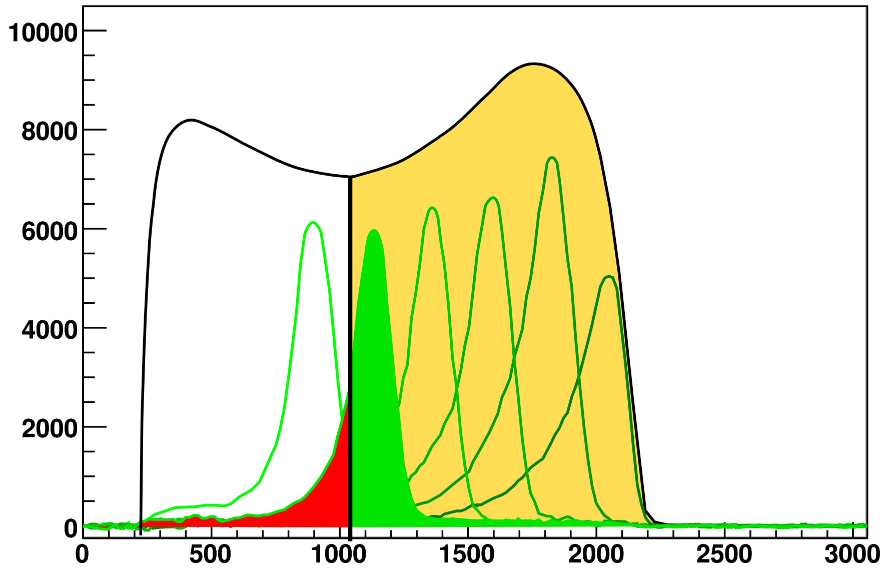

Alternative: **tagged photons**
= quasi-monoenergetic photons

Energy Tagging

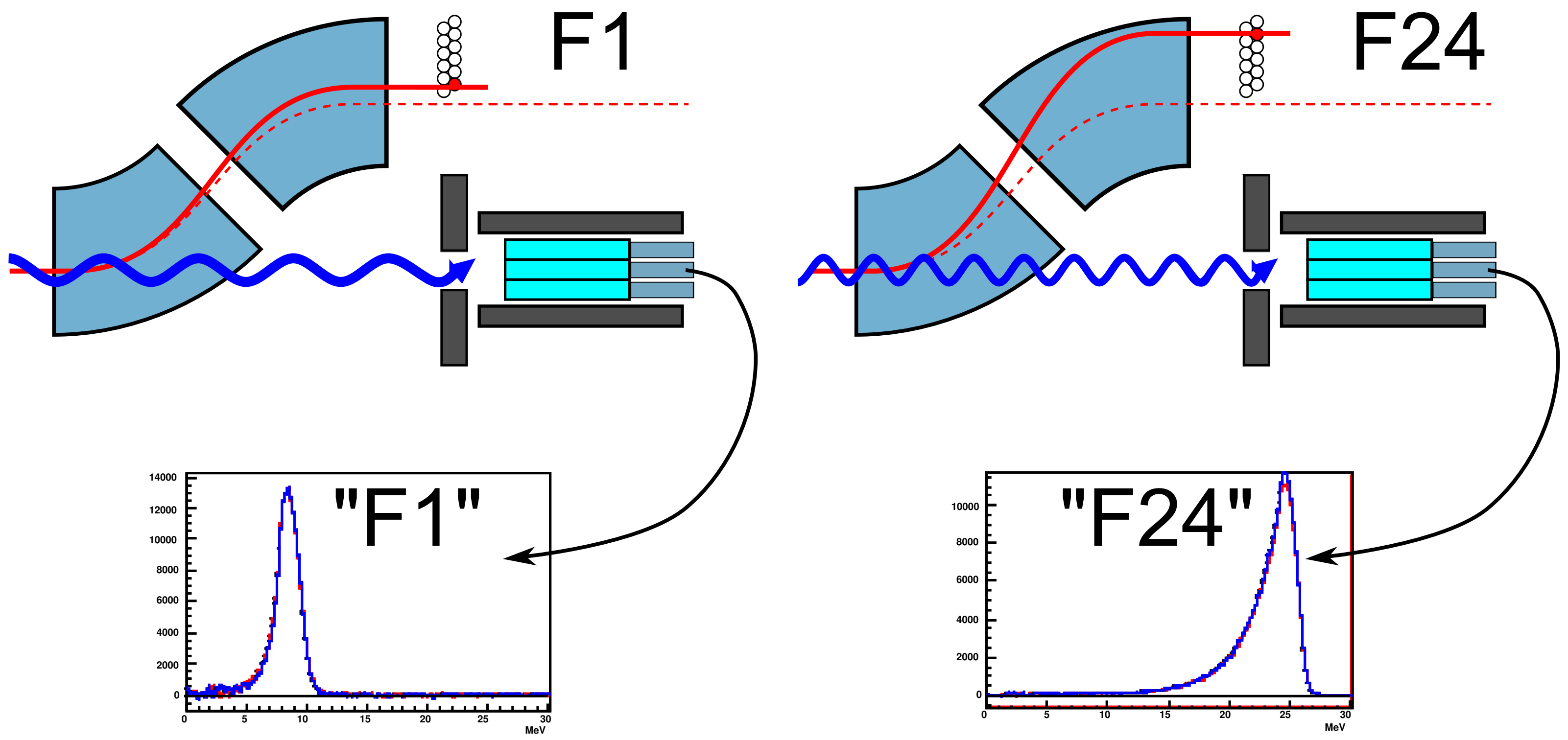

- One photon spectrum for each fiber
- $E_e + E_\gamma = E_{beam}$

Energy Tagging

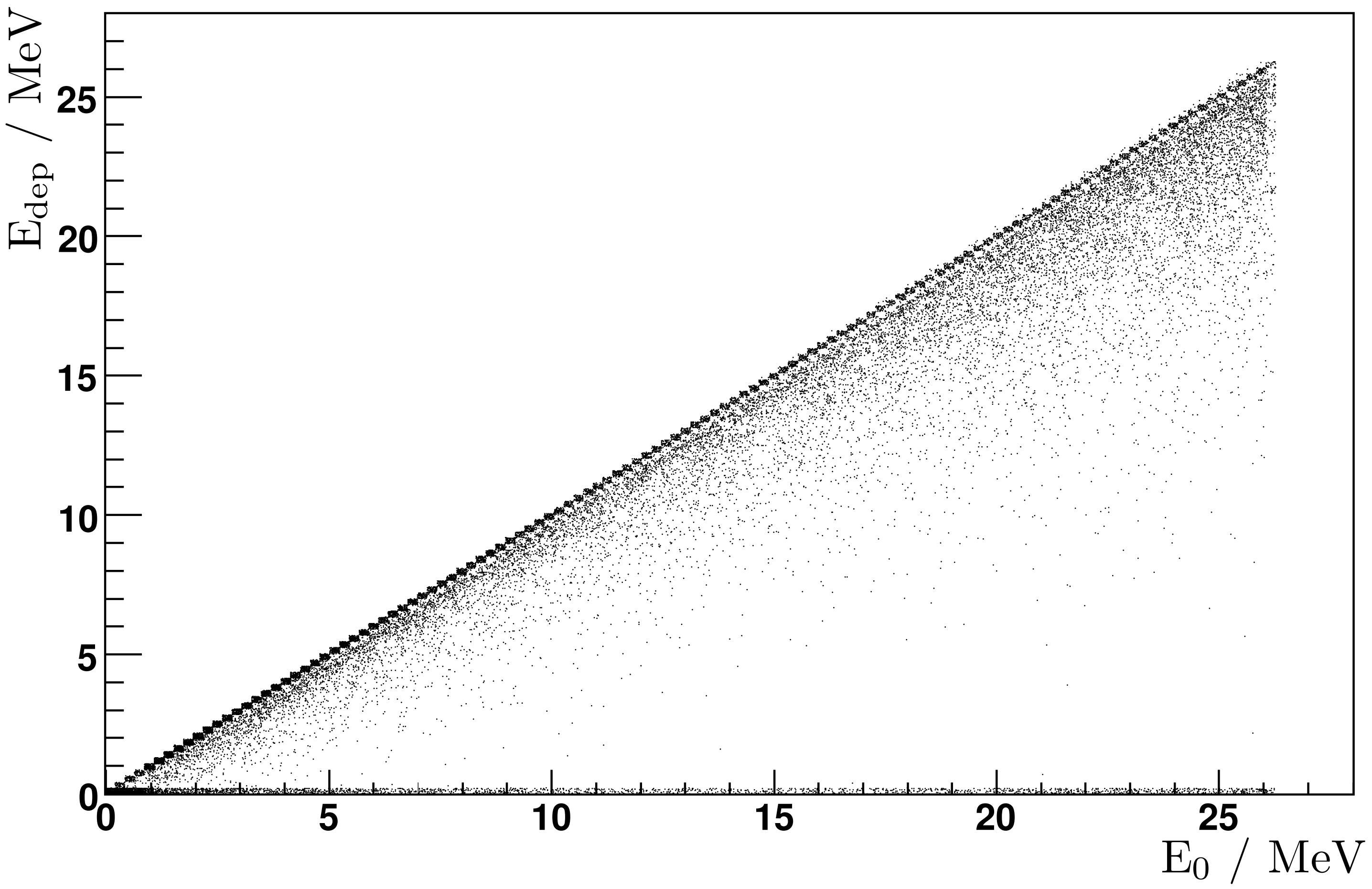

projection from 2dim simulation using $\eta_i(E)$

Energy Tagging

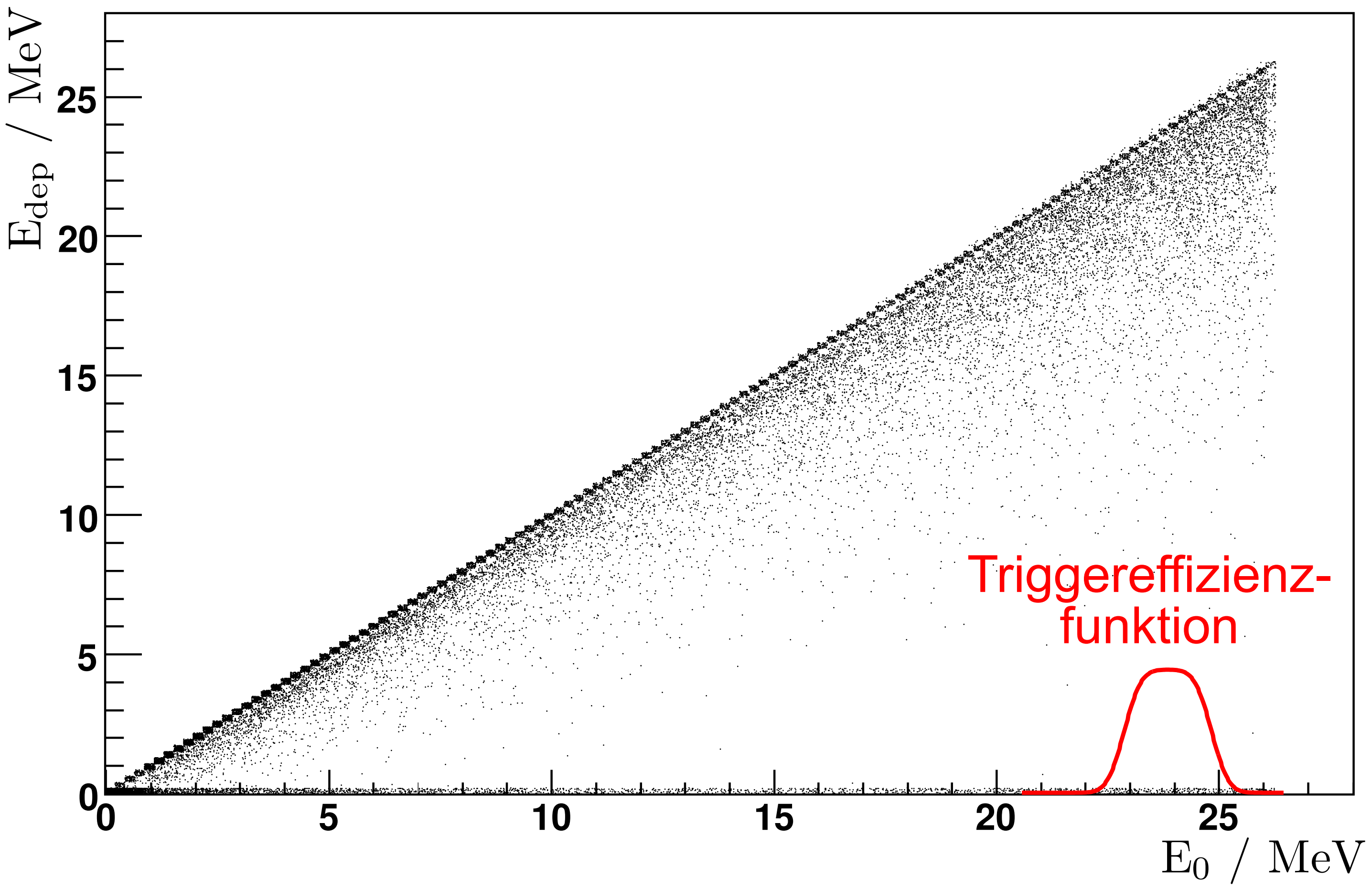

projection from 2dim simulation using $\eta_i(E)$

Energy Tagging

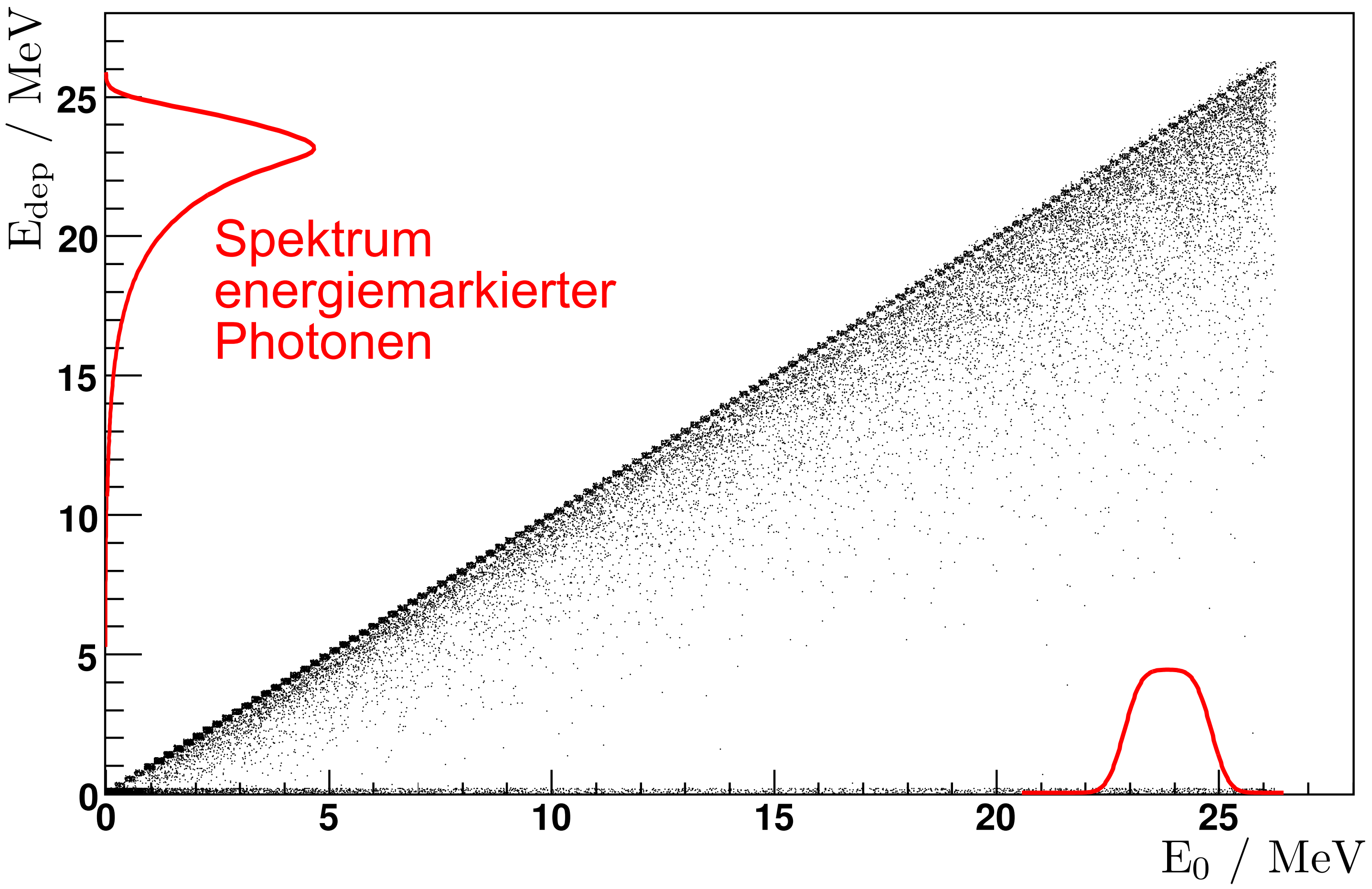

projection from 2dim simulation using $\eta_i(E)$

Energy Tagging

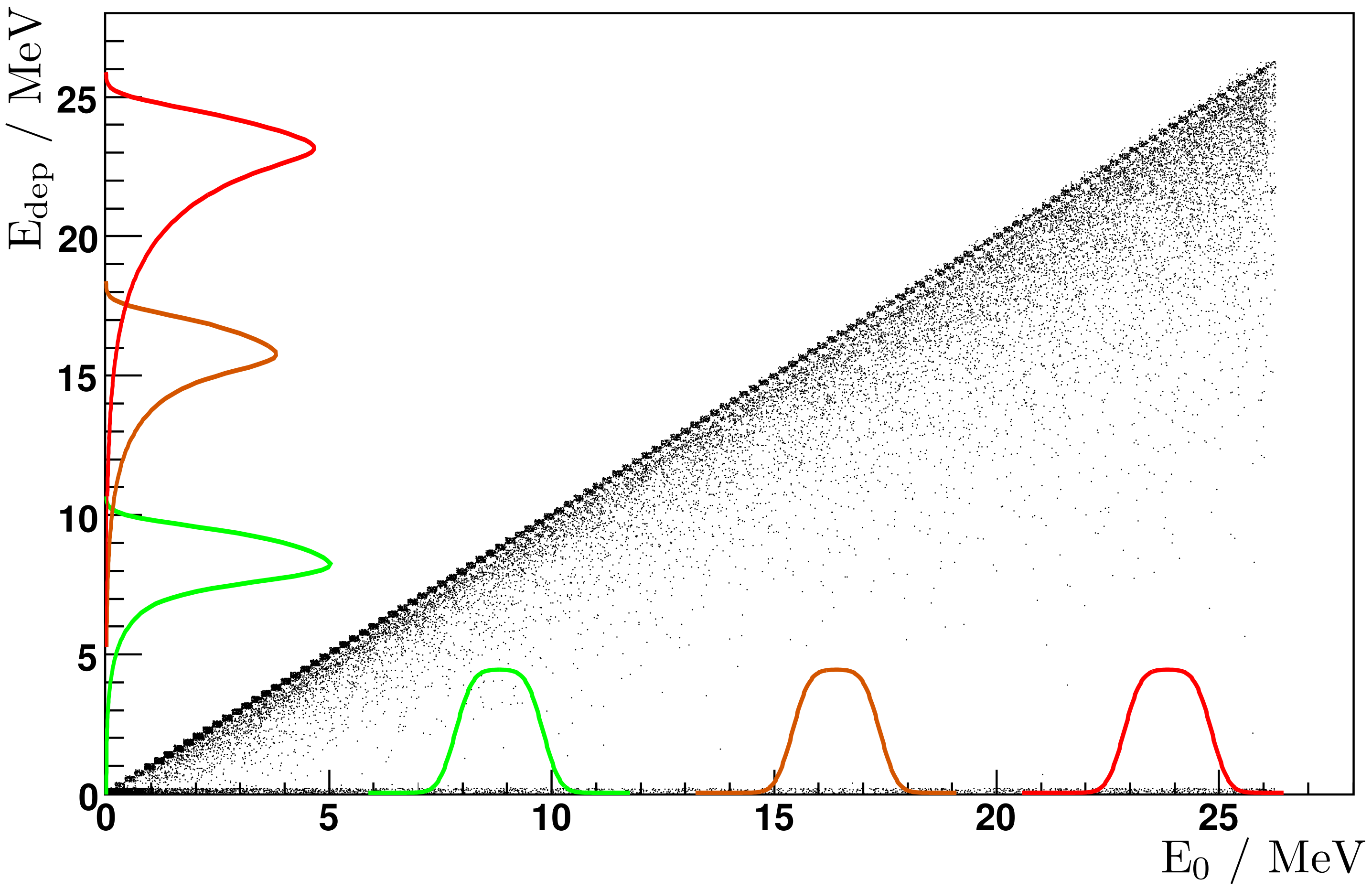

projection from 2dim simulation using $\eta_i(E)$

Simultaneous Fit

set of parameters:

- distance fiber bundle – beam
- dispersion of chicane
- width of Gaussian filter
  (to respect beam position fluctuations etc.)

Simultaneous Fit

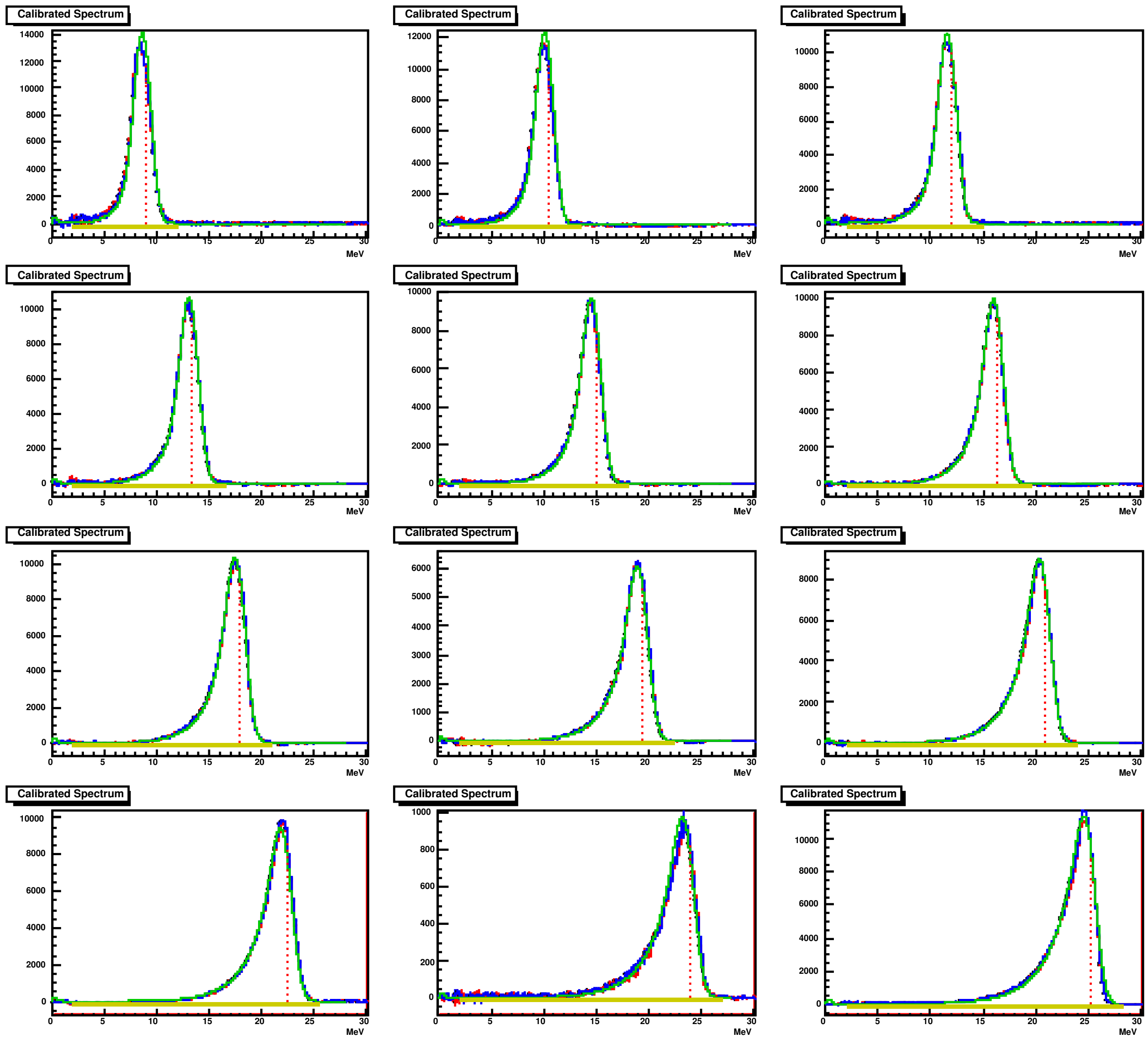

Simultaneous Fit

set of parameters:

- distance fiber bundle – beam
- dispersion of chicane
- width of Gaussian filter
  (to respect beam position fluctuations etc.)

examined sources of errors/applied corrections:

- energy calibration
- dead-time corrections
- pileup (multiple hits)
- random coincidences
- background asymmetries
- analysis thresholds/ranges
- beam energy
- laser wavelength
- geometry of fiber bundle

Results

855 MeV data set: microsample #1

	Wert	**stat.**	**syst.**
polarization product./%	53.24		
correction: dead-time	+0.28	0.10	
correction: random coinc.	+2.24	0.09	
corr. polarization prod.	55.76		
Untergrundnormierung		0.02	
stat. err. (incl. correlations)		4.05	
energy calibration		0.06	
lower threshold (analysis)			0.11
beam energy, laser wavelength			0.00
geometry fiber bundle			0.14
polarization prod./%	**55.76**	**4.05**	**0.18**

Results

855 MeV data set:

$$P_e P_L = \begin{cases} (52.67 \pm 1.15_{\text{stat.}})\ \%\ \text{GVZ OUT} \\ (52.82 \pm 0.92_{\text{stat.}})\ \%\ \text{GVZ IN} \end{cases}$$

for a laser polarization of

$$P_L = (83.5 \pm 1.0)\ \%\ \text{(preliminary)}$$

one gets

$$P_e = \begin{cases} (63.08 \pm 1.38_{\text{stat.}} \pm 1.11_{P_L})\ \%\ \text{GVZ OUT} \\ (63.26 \pm 1.10_{\text{stat.}} \pm 1.11_{P_L})\ \%\ \text{GVZ IN} \end{cases}$$

Outlook

Determination of beam polarization at 1508 MeV:

$$\Delta A_{PV} = \sqrt{\left(\frac{\Delta A_{PV}^{Roh}}{0.80}\right)^2 + \left(\frac{A_{PV}^{Roh}}{P_e^2}\Delta P_e\right)^2}$$

so far $\Delta P_e / P_e = 5\ \%$

$$\Delta A_{PV} = 1.68 \cdot 10^{-6}$$

Outlook

Determination of beam polarization at 1508 MeV:

$$\Delta A_{PV} = \sqrt{\left(\frac{\Delta A_{PV}^{Roh}}{0.80}\right)^2 + \left(\frac{A_{PV}^{Roh}}{P_e^2}\Delta P_e\right)^2}$$

so far $\Delta P_e / P_e = 5\ \%$

$$\Delta A_{PV} = 1.68 \cdot 10^{-6}$$

now $\Delta P_e / P_e = 1.5\ \%$

$$\Delta A_{PV} = 1.19 \cdot 10^{-6}$$

Outlook

Determination of beam polarization at 1508 MeV:

$$\Delta A_{PV} = \sqrt{\left(\frac{\Delta A_{PV}^{Roh}}{0.80}\right)^2 + \left(\frac{A_{PV}^{Roh}}{P_e^2}\Delta P_e\right)^2}$$

so far $\Delta P_e/P_e = 5\ \%$

$$\Delta A_{PV} = 1.68 \cdot 10^{-6}$$

now $\Delta P_e/P_e = 1.5\ \%$

$$\Delta A_{PV} = 1.19 \cdot 10^{-6}$$

29 % smaller uncertainty in ΔA_{PV}, i.e. a factor of 3.3 in ΔP_e

bisher: **5%**

jetzt: **1,5%**

Summary and Outlook

Summary

- Installation of a collinear Compton backscattering polarimeter
- Improvement/development to achieve routine operation
- Energy tagging: Connect data with cross section asymmetry
  $\longrightarrow$ robust basis for data analysis
  $\longrightarrow$ precise measurement of longitudinal beam polarization

Summary

- Installation of a collinear Compton backscattering polarimeter
- Improvement/development to achieve routine operation
- Energy tagging: Connect data with cross section asymmetry
  $\longrightarrow$ robust basis for data analysis
  $\longrightarrow$ precise measurement of longitudinal beam polarization

- **Improvement of $\Delta P_e/P_e$ by a factor of 3.3**
- **Improvement of ΔA_{PV} by presumably 30 % (1.5 GeV, Q^2=0.6 (GeV/c)^2)**

Outlook

- Data analysis for 1508 MeV Compton data still pending... (convergence of simultaneous fits)
- Compton has zero analyzing power for transverse spin so far (no position sensitive photon detector)

$\rightarrow$ *polarimeter for transverse spin:*

- Møller scattering in hydrogen target
- collimator to select θ_{lab}
- dipole magnet to separate Møller from ep, ...
- current/integrating mode detector
- “tracking mode” with plastic scintillators to tune apparatus at low beam current

Diploma thesis, D. Becker

Seemed to work in beam test two weeks ago!

Backup

Faserdetektor

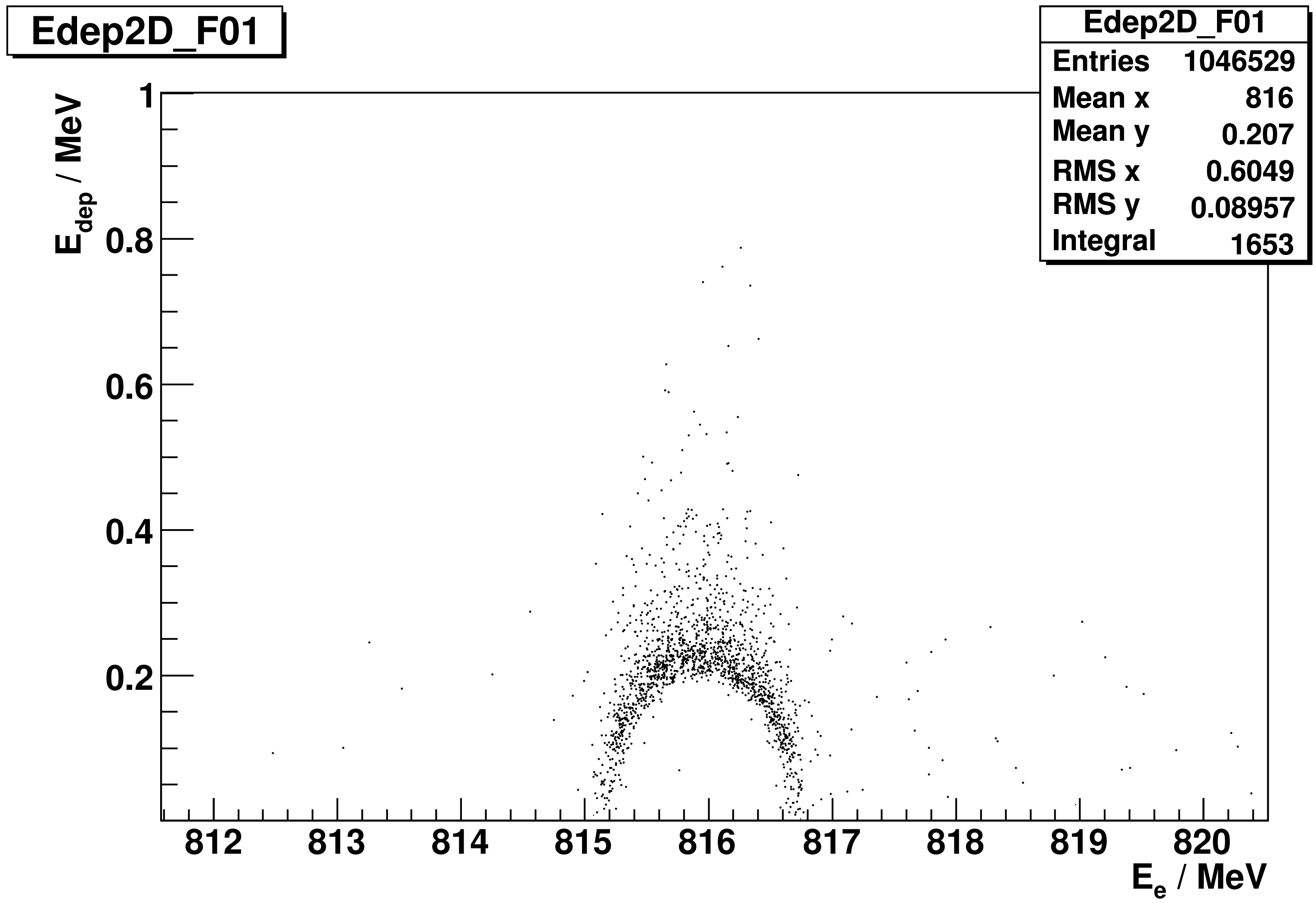

energy deposition in a fiber as function of electron energy

Faserdetektor

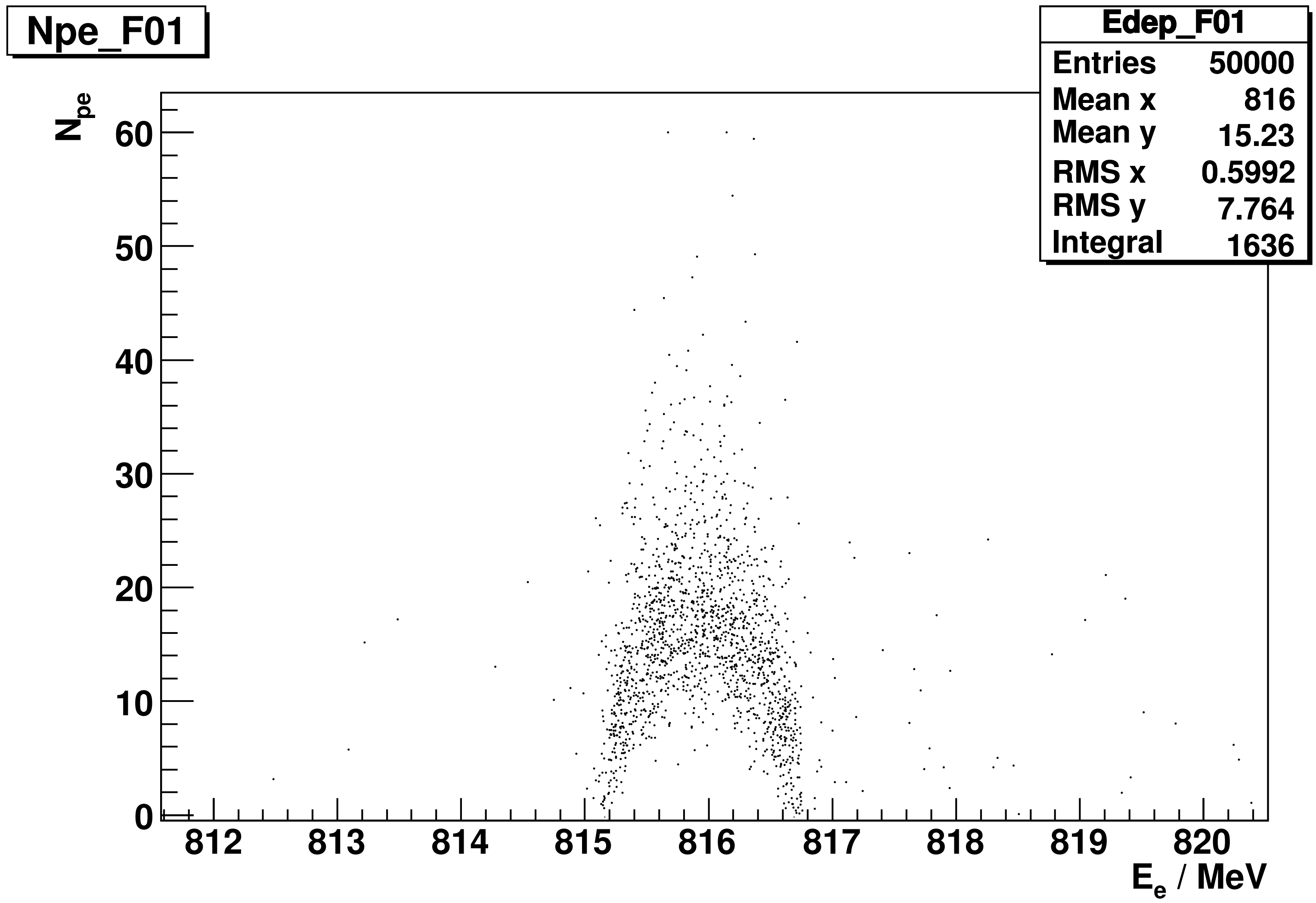

number of photo electrons of a fiber channel as function of photon energy

Faserdetektor

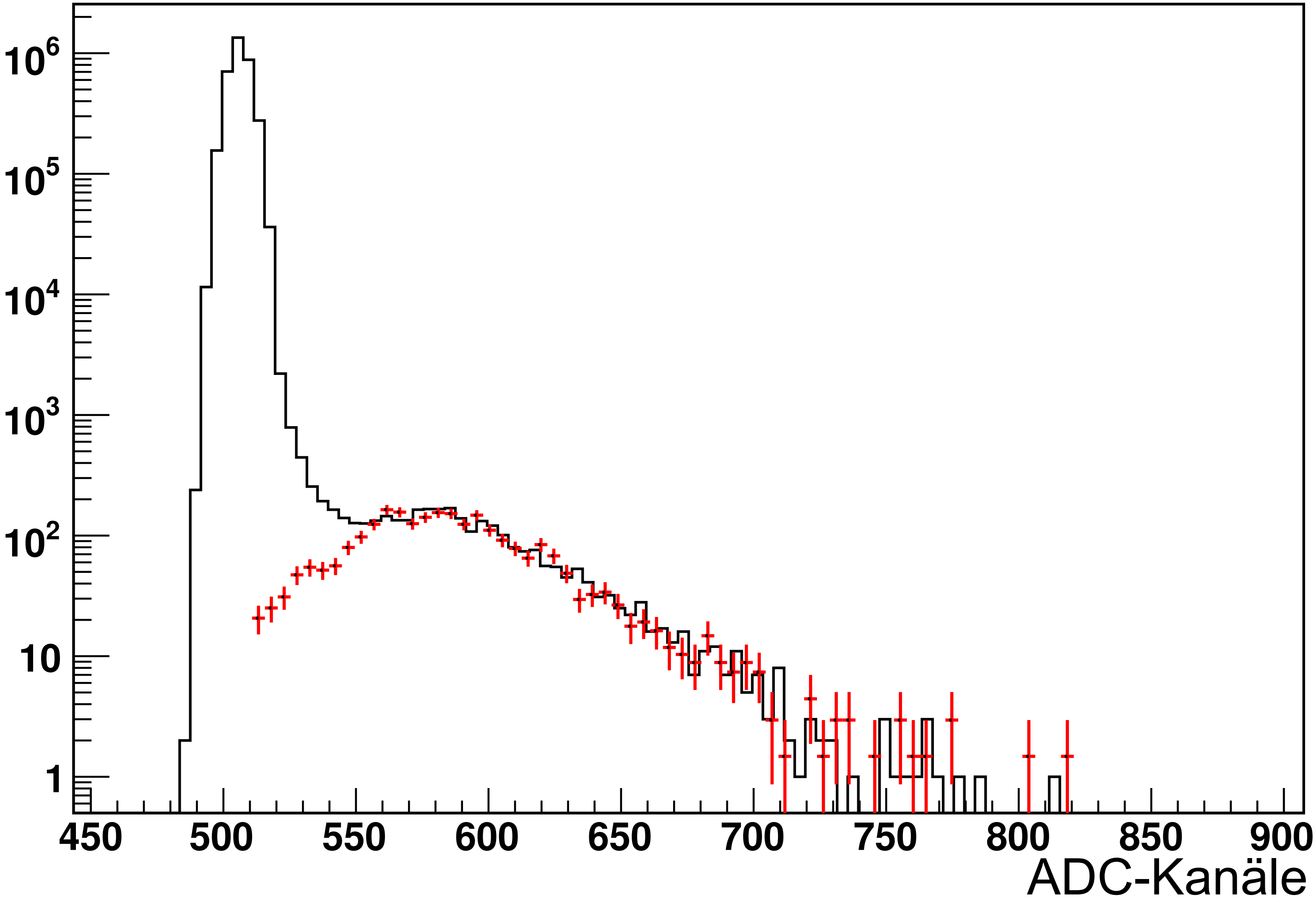

spectrum of photo electrons: **measurement** **simulation**

Faserdetektor

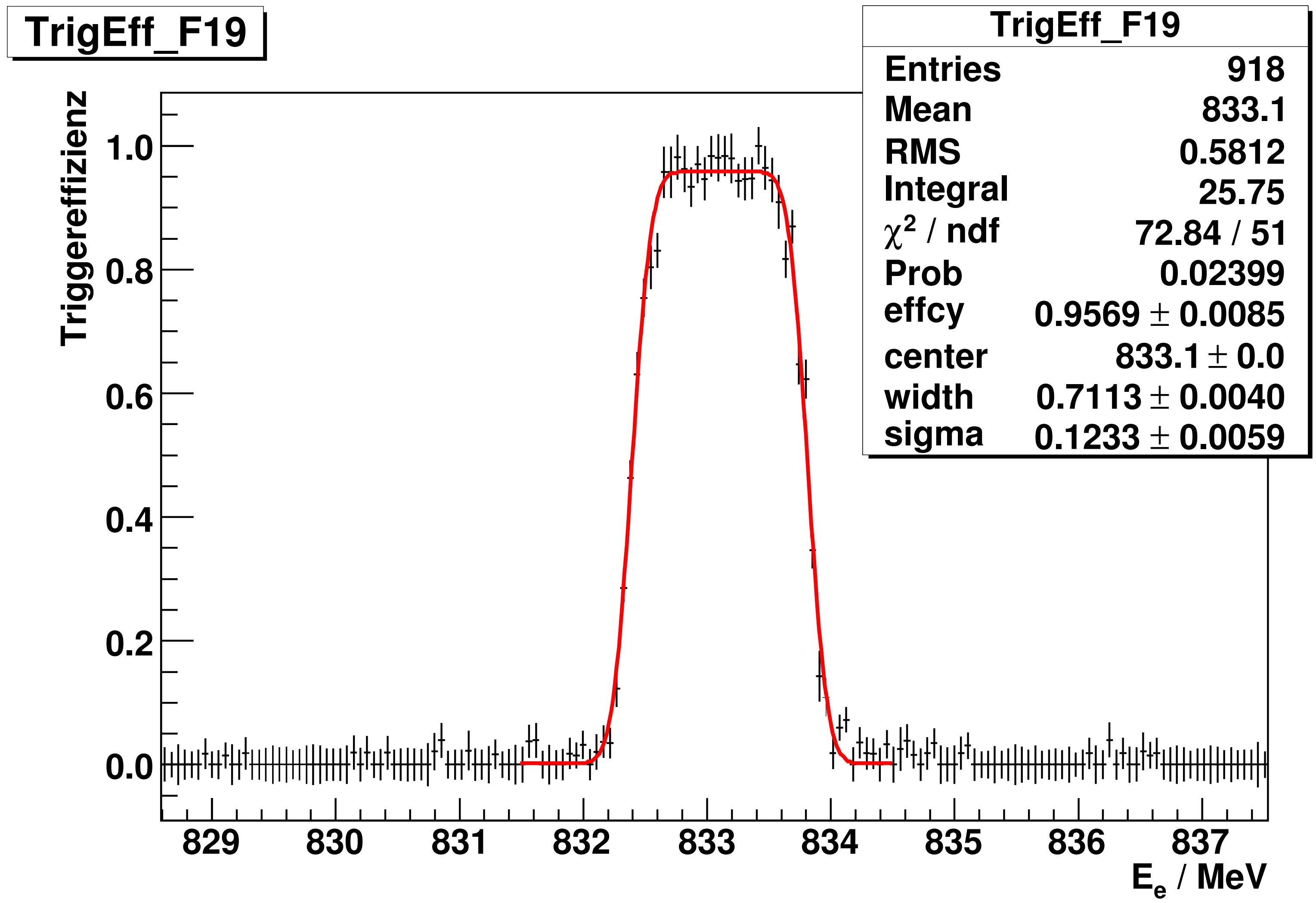

simulated trigger efficiency of a fiber with fitted $\eta_i(E)$

Strange Form Factors at 0,6 $(GeV/c)^2$

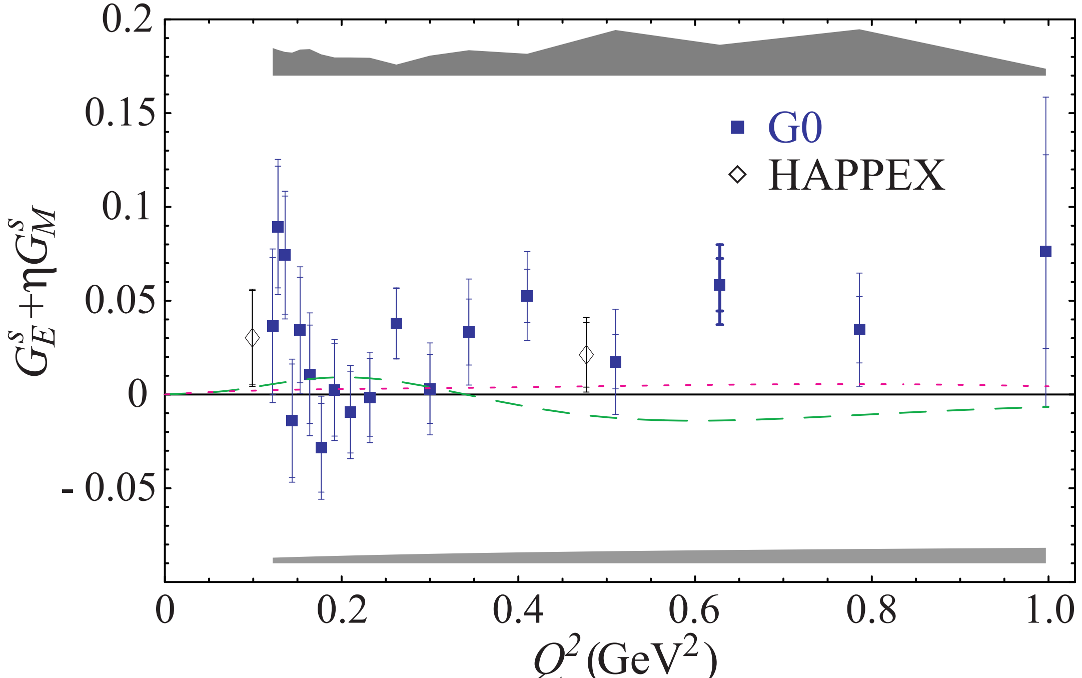

- A4 beam times 2009/2010: $A_{PV} = 23$ ppm, $A_0 = 28$ ppm (preliminary)

- $G_E^S + 0,623 G_M^S = 0,075 \pm 0,026$
- $G_E^S(0,6) = 0 \;\rightarrow\; G_M^S = 0,12 \pm 0,04$

Analysis not finished yet, *small* strangeness contributions possible!

Separation of G_E^S, G_M^S: measurement at 615 MeV, $\theta = 135°$. Impossible due to very high background!?